

AM CVn survey in Astro-WISE

AM CVn survey in Astro-WISE

October 9, 2009

Master thesis by:
Oskar Spooren
Department of Astrophysics
Radboud University of Nijmegen
the Netherlands

supervisor:
dr. G. Nelemans

Department of Astrophysics IMAPP
Radboud University of Nijmegen
Heyendaalseweg 135
6525 AJ Nijmegen
the Netherlands
oskarspooren@gmail.com

Contents

1	Introduction	1
2	AM CVn stars	3
2.1	Stellar Evolution	3
2.1.1	Low-mass stars	3
2.1.2	Mid-mass stars	5
2.1.3	Massive stars	5
2.1.4	Stellar Remnants	6
2.2	Binary star evolution	7
2.3	AM CVn systems	9
2.4	Importance of AM CVn studies	12
2.5	Survey	13
3	Astro-WISE	15
3.1	The path of a photon	15
3.2	What is Astro-WISE?	16
3.3	The Target Processor	16
3.4	From raw data to image	19
3.5	Lists and evaluation	22
4	Analysis	25
4.1	The Data	25
4.2	Median correction	26
4.3	Theoretical Main Sequence and known AMCVn's	27
4.4	Bad fields	28
5	Results	31
5.1	Selection Boxes	31
5.2	The selected objects	32
6	Conclusion	35
A	Astro-WISE scripts	39
B	Candidate Lists	41

Chapter 1

Introduction

For decades now, astronomers have reduced and analyzed the data obtained from their observation runs on various types of telescopes digitally. In these modern days, scientists generally use software packages specifically engineered for their field to obtain the best results. For optical observations in astronomy, the package most widely used for close to twenty years now is called IRAF. Recently people have begun to voice the need for a new package that makes better use of present-day technology, is more user-friendly and is generally better suited to current optical astronomy. One of the resulting software projects is called Astro-WISE. In this thesis, we will use Astro-WISE to (re-)analyze a survey done to find AM CVn systems. AM CVn systems are close binary star systems with helium mass transfer. For more information, see chapter 2.

Astro-WISE is a software package designed for the analysis and subsequent storage of astronomical data, developed by researchers at the Rijksuniversiteit Groningen and others. The Radboud University in Nijmegen, looking to become a partner in this project, has arranged for the Astro-WISE environment to be installed on their own server cluster. This research is meant to test the system in Nijmegen. The goal is both to learn the properties (both advantages and disadvantages) of Astro-WISE and to become able to advise others about its use. For more information about Astro-WISE, please see chapter 3.

The AM CVn survey has been analyzed once before with IRAF. It is a small survey, somewhat of a test, which makes it ideally suited for our purposes. We will be able to obtain the results with Astro-WISE relatively quickly, enabling us to make an assessment of the system without having to go through a too lengthy analyzation process. This does however not mean that the analysis will not be thorough, since we definitely would like to find AM CVn systems that might have gone unnoticed earlier. Apart from the goals relating directly to Astro-WISE, this research is thus also meant to find AM CVn stars in the survey. For more information about AM CVns in general or the methods used to find them, please see chapter 2.

Chapter 2

AM CVn stars

In this chapter I will explain what AM CVn stars are and why we study them. Knowing this, it will be easier to understand why we wish to find more of these objects, which is the aim of this research. A prerequisite of understanding AM CVn stars is of course some basic knowledge of stars and their evolution. A short summary of this subject will also be given in this chapter. For more details, see Prialnik, 2000.

2.1 Stellar Evolution

Stars are born from huge clouds of (mostly) hydrogen gas, called giant molecular clouds. Under influence of the force of gravity, parts of the cloud start contracting and forming clumps. These clumps are large objects composed of gas that can contract due to their own gravity. They are called protostars, the first stage in stellar evolution. These protostars can differ greatly in mass. Some protostars are not massive enough to ever start up the process of fusion. These are called 'brown dwarfs' because they emit very little light. They can remain in existence more or less indefinitely, cooling and emitting less and less light. For the rest of the protostars, their own gravity pushes their gas inward, causing the pressure and temperature in the core of the object to rise so high that the hydrogen there is being fused into helium. From the moment this fusion starts, we call the object a star. The heat that is generated in this process gives the particles more kinetic energy, allowing them to 'bounce' harder off other particles. Also, the radiation generated in the core causes an outward force to emerge. This all generates a pressure that counteracts the force of gravity, stabilizing the star. At this point, the star has arrived at the so-called *main sequence* phase of its life. Depending on the mass of the star, this phase can last between a few million years for very massive stars to hundreds of billions of years for very low-mass stars. The higher temperature and pressure in the cores of more massive stars causes fusion to progress a lot faster, so the more massive a star is, the shorter it will live. The end of the main-sequence phase is signalled when the core of the star runs out of hydrogen. This causes the outward pressure to lower, so the core will start to contract. What happens after this depends strongly on the star's mass.

See Figure 2.1 for a graphical representation of the evolution process.

2.1.1 Low-mass stars

A star of less than about half the Sun's mass (a so-called 'Solar mass') will never be able to fuse the helium in its core even after the core ceases hydrogen fusion. Helium fusion requires a much higher pressure and temperature in the core than hydrogen fusion, and the stellar envelope (the gas around the

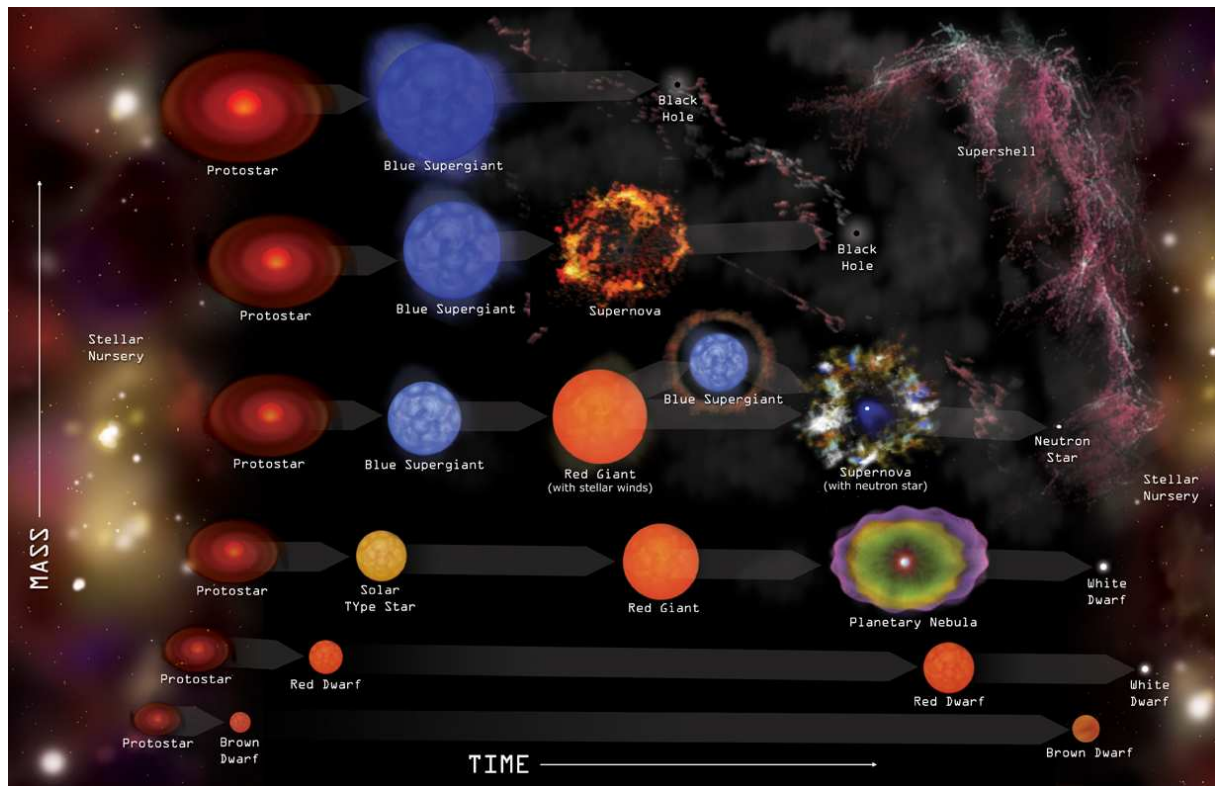


Figure 2.1. Graphical representation of the evolutionary paths of stars.

core) around low-mass stars is simply not massive enough to exert this pressure. These stars are called 'red dwarfs'. Theirs is the second evolutionary path from the bottom in Figure 2.1. They can live in the main sequence phase for thousands of times longer than the sun. This means that, since the known universe is thought to be around 14 billion years old, all the above and following is theory since all red dwarfs are still in their main sequence phase. Eventually though, the hydrogen in their core will run out and fusion stops. The core will contract until the electron degeneracy pressure becomes high enough to halt the collapse.

Degeneracy pressure is a consequence of the so-called Pauli exclusion principle, which states that two fermionic particles (like electrons and neutrons) cannot occupy the same quantum state at the same time. Basically this means that you have to be able to distinguish between the different particles. Particles also have to obey the Heisenberg uncertainty principle, meaning the product of the uncertainty in their position and the uncertainty in their momentum has to be above a certain value. When you compress a material (a gas in the stellar case) very strongly, the uncertainty in the position of the particles has to lower significantly, since because of the Pauli principle particles cannot occupy the same space (for they would then be indistinguishable). This means the uncertainty in their momentum rises. Basically, particles have to have a certain velocity. So, they exert a pressure that is not caused by temperature (like it was when the star was still fusing hydrogen). For electrons, this is called the electron degeneracy pressure. When particles in a material exert more pressure due to degeneracy effects than due to temperature effects, the material is called 'degenerate'.

When the electron degeneracy pressure stabilizes a star, it will turn into a white dwarf. For more information on white dwarfs, see the Stellar Remnants section (2.1.4) later in this chapter.

2.1.2 Mid-mass stars

A star of up to about 2.25 solar masses (Solar type stars, the third evolutionary path from the bottom in Figure 2.1, that can live in the order of billions of years) will develop a helium core that is supported mostly by electron degeneracy pressure (less so the more massive the star is), while hydrogen fusion still goes on in a layer immediately over the core. This fusion goes on in an accelerated manner because the gravity of the core increases the pressure on these layers, and causes the star to expand. Since the outer layers are lifted away from the core, thus reducing the gravity on them, the expansion goes faster than the energy production increases. As such, the expanding stellar envelope cools, causing the star to become redder than it was on the main sequence. Stars such as this are known as 'red giants'. The hydrogen around the core is fused into helium, the latter being subsequently absorbed by the core. This causes the core to contract even further, which makes the hydrogen fuse faster. Eventually this leads to the ignition of helium fusion in the core. In stars below about 2.25 solar masses, the core is degenerate, so that the pressure is influenced only very weakly by the temperature. This means that the helium fusion can become a runaway process, resulting in a so-called helium flash. This greatly increased energy production causes the temperature to rise to a level that thermal pressure once again becomes dominant. Helium burning then proceeds normally. For stars between 2.25 and about 8 solar masses, helium fusion starts before the core becomes degenerate. They evolve along similar paths, only lacking a helium flash.

The energy released by the helium fusion causes the core to expand, so that hydrogen fusion in the overlying layers slows. The total energy generation decreases, since helium fusion is far less efficient than hydrogen fusion, and the star as a whole starts to contract. It does not shrink back to its original size on the main sequence, but does gradually decrease its radius and increase the temperature on its surface. After the star has consumed the helium in the core, a shell of helium around the hot carbon and oxygen core continues the fusion and once again causes the star to become a red giant, similar to before yet shorter-lived.

Helium burning reactions are extremely sensitive to temperature, causing great instability. The pulsations that results from this can give the outer layers of the star enough kinetic energy to be ejected. An expansive shell is build up around the stellar core, which cools and starts to form dust and molecular particles. This envelope is called a 'planetary nebula'. At the centre of the nebula remains the core of the star, which cools down to become a white dwarf. See Figure 2.2 for a picture of a planetary nebula.

2.1.3 Massive stars

Massive stars are very bright, hot and large in their main sequence time, causing them to be a blue colour. They are called 'blue supergiants' for this reason. They can live hundreds of millions of years for the less massive of this group, down to only a few million years for the most massive. The three top paths in Figure 2.1 are theirs, in decreasing mass from top to bottom. While they brighten less during their red giant phase than mid-sized stars (since helium fusion starts up sooner) they are still much brighter than the latter in this phase and are thus known as 'red supergiants'. Extremely massive stars (above about 40 solar masses) have very strong *stellar winds*. Stellar wind is a name for the mass loss of a star caused by radiation pressure. These extremely massive stars lose mass so rapidly due to these winds that they tend to strip off their own envelopes, causing them to retain their high surface temperature and remain



Figure 2.2. The Cat's Eye Nebula. This is a planetary nebula caused by the death of a star with about the same mass as the Sun.

blue, or become blue again after having been red for a period of time. Stars cannot have a mass of more than about 120 solar masses since the outer layers would be expelled by the extreme radiation.

The core of a massive star grows continually hotter and denser as it gains material from the fusion of hydrogen in the lowest layer of the envelope surrounding it. The high temperatures in the core cause the gas pressure to be more important than the electron degeneracy pressure. However, both combined are insufficient to halt the collapse, so the core can continue to contract. After helium fusion, carbon fusion will start up, and after this progressively heavier elements, each temporarily halting the collapse. Once this process reaches iron, however, there can be no energy gained from fusion anymore. The core will undergo a sudden, catastrophic collapse. In a process that is not yet completely understood, a lot of the energy produced in this collapse is used to throw the material in the outer layers outward in shockwaves. This is called a *supernova* (type Ib, Ic or II, depending on the exact composition of the star). For stars originally of a mass of around 20 solar masses or less (this limit is still very unsure), the neutron degeneracy pressure in the core (similar to the electron degeneracy pressure) stabilizes the star, forming a neutron star. For stars more massive than this, even this pressure is not enough to halt the collapse and it will continue all the way to a black hole. For the latter, it is not even sure if a supernova always proceeds this collapse. For more information about both of these, see the Stellar Remnants section (2.1.4) next.

2.1.4 Stellar Remnants

As discussed above, there are three possible stellar remnants. White dwarfs, neutron stars and black holes. White dwarfs are stellar cores compressed into about the volume of the Earth. The inward pull of gravity is balanced by the degeneracy pressure of the star's electrons. White dwarfs of higher mass have

a smaller volume. White dwarfs have no fuel left to burn, so they slowly radiate away the heat it has left. In the end, all that remains is a dark mass that sometimes is called a 'black dwarf', although the universe isn't old enough for any of these to exist yet.

When a massive stellar core collapses, the pressure causes protons and electrons to form neutrons via a process called electron capture. Most of the core of the star becomes a dense ball of neutrons, with a thin overlying layer of degenerate matter. The neutrons resist further compression the same way electrons do in white dwarfs, via the neutron degeneracy pressure. Neutron degeneracy pressure is stronger than electron degeneracy pressure. The resulting stable objects are called neutron stars. They are extremely small, with a radius of about 10 km.

If the mass of the stellar remnant is high enough, even neutron degeneracy pressure is not enough to halt its collapse. The stellar core will collapse into a black hole. Black holes are predicted by the theory of general relativity. No matter or information can flow from the interior of a black hole to an outside observer. Their existence is however well supported, both by theory and observations. While they themselves emit no light, the effect of their mass on other material or stellar bodies nearby can be observed.

2.2 Binary star evolution

So far we have only discussed single stars. However, two thirds of all stars are born in so-called *binary systems*. We will give a summary on binary stars here (for more details, see for example Hilditch, 2001). A binary star is a star system consisting of two stars orbiting around their common center of mass. The more massive of the two stars is called the primary, the other is its companion star or secondary. Binary stars are formed through fragmentation of the molecular cloud during the formation of protostars. Binary star evolution is different from single star evolution since the components of a binary star system can influence each other's evolution, depending on their relative size, mass and distance.

Binary star systems can be assigned to three different classes, depending on the distance between the stars, their mass and their size. These three factors determine the so-called *Roche Lobe* of each component. The Roche Lobe of a star is the area in which the matter will stay gravitationally bound to that star. Meaning, if the star outgrows its Roche Lobe, its matter will start flowing to the other star, or even leave the system completely. See Figure 2.3 for a graphical representation of this concept. The size of both stars compared to the size of their Roche Lobe determines which of the following three classes a binary system belongs to:

- *Detached binaries* are binary stars where each component is within its Roche Lobe. The stars have no major effect on each other and essentially evolve separately. Most binaries belong to this class.
- *Semidetached binaries* are binary stars where one of the components fills its Roche Lobe while the other does not. Gas from the surface of the Roche-Lobe-filling component (called the donor) is transferred to the other star (called the accretor). It can either impact directly on the surface of the accretor or form a so-called accretion disc around it (see below).
- *Contact binaries* are binary stars in which both components fill their Roche Lobe. The uppermost layers of both stars form a common envelope that surrounds both stars. The friction caused by the cores moving through this envelope brakes the orbital motion, such that both stars may eventually merge or the envelope is expelled.

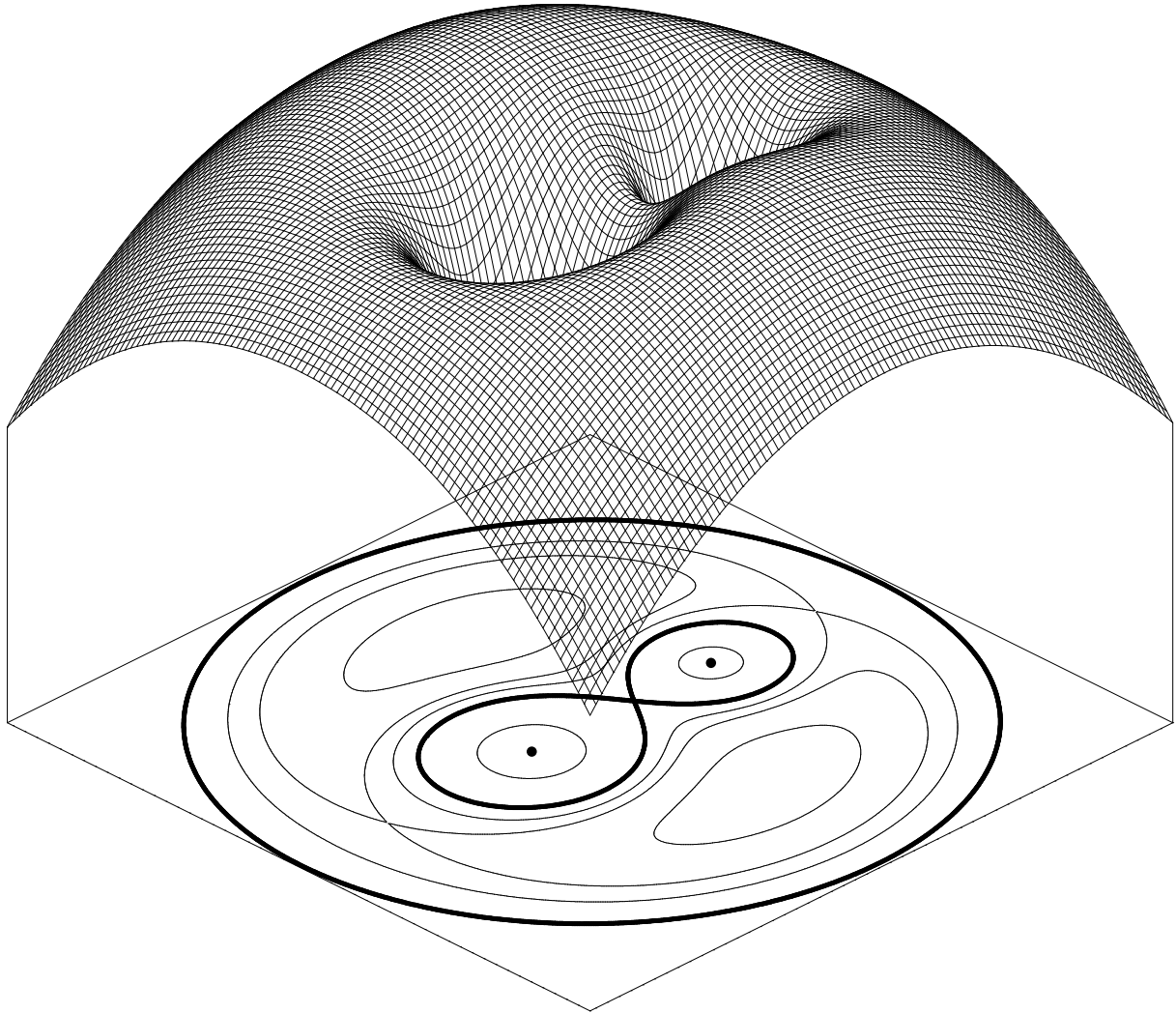


Figure 2.3. Graphical representation of the Roche Lobe concept. In the 2D picture, the black dots are the centres of mass of the two stars. The thick, black, 8-shaped line marks the outer edge of their Roche Lobes. Any mass going over this line will either get pulled to the other star or leave the system completely. In the 3D picture, which shows the gravitational potential, the two pits represent the Roche Lobes of the stars. Any particle going out of a pit will either fall into the other one or roll out of the system.

The term *accretion disc* was mentioned in the explanation of semidetached binaries above. An accretion disc is a phenomenon caused by the law for conservation of angular momentum. Angular momentum is a measure for the amount of rotation a mass or particle has. The law for conservation of angular momentum states that it must be conserved in a closed system, like a binary star where mass is not lost to outer space. To conserve angular momentum, mass moving from the donor star might be unable to directly impact upon the accretor, especially if the latter is a compact object such as a white dwarf. Instead, it orbits the accretor in a position that follows from the amount of angular momentum it has. Viscosity in this matter can transfer angular momentum between the particles in it, making some able to accrete upon the surface of the star and others move out further, thus creating a disc. Such a disc can

be stable, which means it will deliver mass to the star in a constant rate, or unstable, meaning it delivers the mass in irregular batches.

Binary stars start as detached binaries, two main sequence stars that evolve more or less separately. When one of the stars evolves to a red giant however, the binary can become semidetached and mass transfer will start to dominate the evolution of both stars. This can lead to scenarios that are not possible in single star evolution. For example, in the *Algol* system the more massive component is still in the main sequence, while the less massive companion is at a later evolutionary stage. This might appear strange, since components of a binary star form at the same time and massive stars evolve faster than less massive ones. The paradox can be solved by taking mass transfer into the equation: when the more massive star became a giant, it filled its Roche Lobe and most of the mass was transferred to the other star, which is still in the main sequence.

There are many possible evolutionary paths for a binary, and we will not discuss all of them here. One interesting case is a *Cataclysmic Variable*, where one of the stars in the system is a white dwarf. It accretes matter from the other (donor) star, via an accretion disc. This accretion disc is unstable, causing matter to fall in to the white dwarf irregularly. This matter is composed mainly of hydrogen. When a certain amount of matter is compressed onto the surface of the white dwarf, it can reach the threshold for hydrogen fusion and suddenly ignite, burning up the outer layer of hydrogen. The sudden brightening of the system due to such an event has given it the name of *nova*, as the bright system can appear as a new star (nova) in the sky. The white dwarf may get more massive due to this process, and if it gets too massive it can reach the threshold for carbon fusion. Fusion in a degenerate object is a runaway process, so it will disrupt the entire white dwarf in a huge explosion. This is called a type Ia supernova.

One possible path for a binary to follow is most interesting in our case. It is possible that when the more massive star of a binary swells up to a red giant and overflows its Roche Lobe, the resulting mass transfer to the less massive star causes a runaway process that further enlarges the giant. Eventually, both the core of the giant star and the secondary star will be engulfed in the mantle of the giant, which has become a common envelope. While the exact progression of this phase is as of yet unknown, we do know that the friction brakes the orbital motion and this can either cause the stars to merge, or the entire envelope to be expelled. In the latter case, we are left with a binary system in which the two stars are very close together, also called a *compact binary*. One type of compact binary is an AM CVn star, which are at the center of this research.

2.3 AM CVn systems

The abbreviation AM CVn star stands for AM Canum Venaticorum star. This is because the variable star AM in the constellation Canes Venatici is the prototype of this category. Originally, this star was catalogued as a faint blue star with exclusive helium absorption lines featuring peculiar shapes in its spectrum (Greenstein & Matthews, 1957). The spectrum of a star shows the amount of radiation it emits in each different wavelength. In general, a star's spectrum is continuous. If for example the star has an outer layer of hydrogen, this hydrogen would absorb certain wavelengths of the radiation emitted, causing so-called *absorption lines* in the spectrum. If the star for example has an accretion disc of hot hydrogen, this hydrogen could emit radiation as well, causing *emission lines* in the spectrum. So, the different lines in a spectrum can tell us something about the composition of the star system it originates from. The (time dependent) shape of the lines can provide information on the parameters of the system, such as the orbital period in a binary system. The fact that AM CVn has exclusive helium absorption lines with peculiar shapes hints that the mass transfer in the object is composed mainly of helium and it

has a configuration we cannot readily identify.

Later, variations were detected in the AM CVn lightcurve (Smak, 1967). A lightcurve shows the total amount of light emitted by a star over a period of time. Variations in the lightcurve mean the star has a variable light output towards us observers. This can be because the star itself is variable, for instance because it oscillates in radius, or because the star is actually a binary star system. In the latter case one of the stars can temporarily obscure the other, causing a drop in the light that reaches us. It was suggested that AM CVn is an ultracompact binary star consisting of two degenerate objects (like white dwarfs). On account of 'flickering' in the lightcurve it was proposed that the binary also transferred mass (Warner & Robinson, 1972). This is because mass transfer is generally not entirely stable, so the light generated in this process is variable. Conclusive evidence for the binary nature of AM CVn was only obtained in 2001 from a technique called Doppler tomography, which validated the assumption that AM CVn is an ultracompact binary consisting of two degenerate objects (Nelemans et al., 2001). Doppler tomography is a technique for making two-dimensional images of point sources such as compact binaries, which we will not explain further here.

Today, AM CVn stars are defined as binary systems that have very short orbital periods (less than about an hour) and helium dominated spectra (Nelemans, 2005). Mass transfer occurs in these systems, which is driven by angular momentum loss due to gravitational wave radiation. Gravitational wave radiation is a phenomenon that occurs when two masses orbit around each other. It is predicted by the general theory of relativity. Basically, the rotation of two masses orbiting around each other causes ripples in space. Important for us is mostly the result: energy and angular momentum is carried away from the system. The closer the masses are together and the heavier they are, the more effective is this outflow of energy and angular momentum due to gravitational wave radiation. Since the distance between the two masses is related to the orbital period of the system in such a way that larger distances mean larger orbital periods (this is called Kepler's Third Law), smaller orbital periods mean *more* gravitational wave radiation. Because the loss of energy and angular momentum causes the orbital period to decrease (so the stars come closer together), gravitational wave radiation can cause an inspiral that can end with the merger of the two objects. However, in AM CVn systems, at a certain point the stars will start to transfer mass. Since mass transfer in this case, due to conservation of angular momentum, actually causes the orbital period to increase, this makes the situation more complicated. The gravitational wave radiation is pushing the orbital period down, while the mass transfer is increasing it. Without the gravitational wave radiation, mass transfer could eventually stop because the donor's Roche Lobe would outgrow its size. So, the mass transfer is actually driven on by the gravitational wave radiation.

In the end, gravitational wave radiation and mass transfer together cause the system to evolve to longer orbital periods. As far as we can tell from the currently known AM CVn stars, this evolution takes the system through three distinct phases (Tsugawa & Osaki, 1997). Firstly, a high-state phase (periods below about 20 minutes) during which low-amplitude photometric variations can be seen on various periods. Systems in this phase are characterised by broad, shallow helium absorption lines. Secondly, an outbursting phase (periods between about 20 and 40 minutes) in which large optical variability can be seen. During the bright phases these systems resemble high-state systems, while emission lines are visible during the quiescent phases. The outbursts are probably caused by an unstable accretion disc, like in the case of the Cataclysmic Variables explained in the previous section. The third phase (periods above 40 minutes) features systems that show no optical variability, which means they probably have stable, cool accretion discs. This can be seen by helium emission lines in the spectrum.

It is still unknown how AM CVn systems are formed. We do know that the accretor is a white dwarf and the orbital period is relatively small, so the stars are close together. The spectra of the AM CVn stars further show that the transferred material is mainly composed of helium. There are three proposed

routes for the formation of AM CVn's, which for the currently observed systems are in principle all viable (see Nelemans, 2005):

- The first one features detached close double white dwarfs which lose angular momentum due to gravitational wave radiation, evolving to shorter and shorter periods, and are thus brought into contact. The less massive white dwarf starts transferring mass (since this is the larger of the two and will fill its Roche Lobe sooner) and if the white dwarfs don't subsequently merge, an AM CVn star is born. This star then evolves to longer periods with an ever-dropping mass-transfer rate.
- In the second possibility a low-mass, non-degenerate helium burning star transfers mass to a white dwarf companion. This star is basically a mid-sized star that has already exhausted the hydrogen in its core and has moved on to helium burning. The star has lost its hydrogen due to mass transfer already. Mass transfer has also prevented it from becoming a red giant (since the mantle was lost). If this star and the white dwarf are close enough, transfer of helium can start before the non-degenerate star has exhausted the helium in its core. The system will evolve through a period minimum of about ten minutes. After this, the period will start to increase again with a strongly decreasing mass-transfer rate. This explains the formation of an AM CVn star.
- The third formation channel starts with a Cataclysmic Variable. If the secondary in this system is evolved (meaning it has exhausted the hydrogen in its core) and mass transfer has uncovered its helium-rich core, they can evolve rather similarly to the helium star tracks of the second formation route.

In Figure 2.4 the path each formation channel follows in term of mass transfer rate and orbital period is shown. To distinguish between the different scenarios, more information is needed, such as the chemical composition of the donor star (Nelemans et al., 2009).

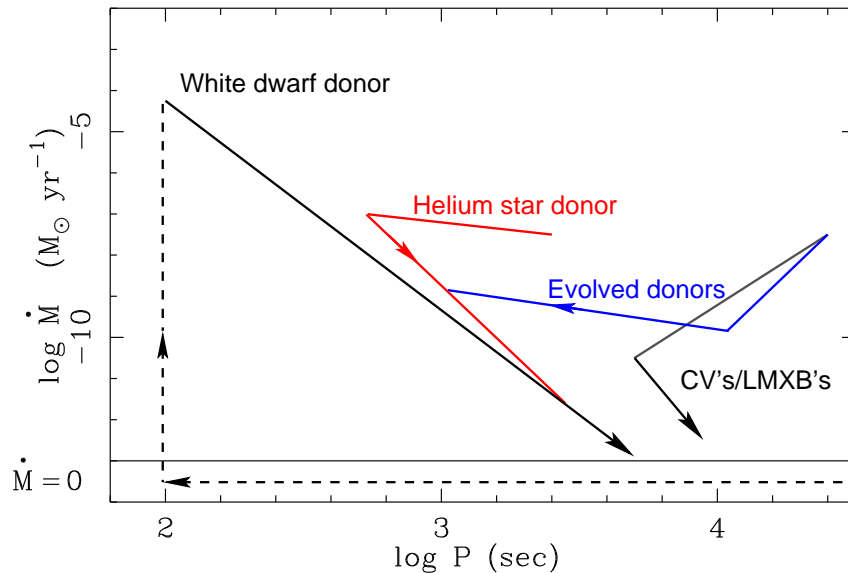


Figure 2.4. Evolutionary tracks followed by an AM CVn for each possible formation scenario. On the y-axis, the logarithm of the mass transfer rate is shown. On the x-axis, the logarithm of the orbital period is shown. As can be seen, in the end all AM CVns evolve to longer periods with an ever-decreasing mass transfer rate. It is also clear that simply knowing the orbital period, and even knowing with some certainty the mass-transfer rate as well, is not enough to distinguish clearly between the different scenarios.

2.4 Importance of AM CVn studies

AM CVn stars are interesting objects because of their short periods and the fact that donor stars in these systems have peculiar chemical composition. Since the spectrum shows that no hydrogen, but helium, is transferred to the accretor, this means the donor star must have been somehow stripped of its hydrogen. Both the short periods and these interesting donor stars constitute a special environment where we can study astrophysical processes. An example of this is the physical nature of Helium accretion discs, of which we know very little. Helium dominated accretion discs are unique to AM CVn stars. It is expected that the gravitational wave radiation driven mass-transfer drops by at least five order of magnitude over the observed period range. This would allow the study of Helium accretion discs as function of mass-transfer rate. As already mentioned, AM CVn stars probably go through three phases in their evolution, as do their Helium accretion discs. They go from stable and hot, to unstable, to cool and stable. To this date, very few models for Helium accretion discs are in existence (see for example Tsugawa & Osaki, 1997). All other known accretion discs in the universe are hydrogen dominated. All theory on accretion discs is based on these hydrogen accretion discs. Since helium has a very different ionization temperature than hydrogen, effects like the viscosity in the disc are expected to behave differently. The study of helium accretion discs can be an independent experiment to confirm our theories on accretion discs are in fact correct and valid for different types of discs.

Many questions about AM CVn stars themselves are unanswered, of which one of the bigger ones is how they are formed. One of the possible ways to distinguish between the different formation channels is to look at the chemical composition of the donor star (via the accretion disc). In case the donor is a white dwarf, it should show a helium white dwarf or carbon/oxygen white dwarf composition. The helium star channel descendants should show produces of helium burning and the CVs with evolved donors can show traces of hydrogen. Currently, only helium and nitrogen have been found. This is insufficient to rule out any of the three routes. At the moment, only about 20 AM CVn systems are known. We need more systems to study if we are to find any statistically relevant evidence that can confirm or rule out any formation route.

At the moment, we don't know the Galactic population of AM CVn systems. We have some predictions as to how many to expect (between 10 million to more than 100 million, see Nelemans 2005), but they are very uncertain, mainly because the efficiencies of the different formation scenarios are not well known. These predictions however suggest that there are many more relatively bright longer period systems undetected (hundreds, at the least). The exact population of these systems is important to answer the question of the formation of AM CVn systems. If one formation channel is very inefficient for instance, and we were to know there are a lot of AM CVn systems out there, it is unlikely this formation process is the only one responsible for AM CVn stars. On the other hand, we could for instance find out all known AM CVn systems have a certain chemical composition of the donor star corresponding to one formation channel. If we would then also know these systems constitute 10% of the total population, we could be relatively sure we have found the correct formation channel. Should we only know 1% of the population though, this prediction would be most uncertain. Also notable is that AM CVns are the only known sources of gravitational wave radiation in their frequency band (e.g. Hils et al, 2000). This means they will likely be detected by the future LISA space mission, which is a mission aimed at detecting these gravitational waves. Knowing the population of AM CVn stars in the Galaxy, we would be able to predict how much gravitational wave radiation from these sources LISA will detect, which will help sort the myriad of data this mission will generate. To predict the population of AM CVn systems in the Galaxy with more certainty, more data, in the form of more systems found, is needed.

All in all, finding more AM CVn stars is important if we are to understand them. It is also important for our understanding of certain astrophysical processes in general, such as the physics of accretion discs

and the spectrum of gravitational wave radiation.

2.5 Survey

As established in the previous section, we need to find more AM CVn systems. The question is: how do we accomplish this? To answer this we need to look at the distinctive properties of AM CVn stars, specifically those that would show in observations. An AM CVn is a rather blue object with helium emission or absorption lines, lacking hydrogen lines. Most of its life is spent in the phase with helium emission lines. Those helium emission lines, not accompanied by hydrogen lines, are unique to AM CVn systems and are thus a good way to find and identify them (helium absorption is very weak and thus not a reliable way for identification). When looking at the spectrum of an AM CVn star, it would be readily identified by these distinct helium emission lines and the absence of hydrogen features. The most reliable way to find AM CVn systems would thus seem to be to simply take spectra of stars and go through them. However, both recording the spectra and the subsequent analysis are painstakingly slow processes. Considering the amount of visible stars in the Galaxy, this method is not feasible on such a large scale.

Next to taking spectra of sources however, it is also possible to simply make a photograph of a section of the sky. This would give us information about the brightness of the stars in that part of the sky. Filters are used to select only a specific portion of the radiation that the sources emit. Normally, different colour filters, such as blue and red, are used when making a photometric observation. These filters are broad, letting through the light of a big portion of the spectrum. For the purpose of finding AM CVns, narrow filters can be used that for example let through only that part of the spectrum where a helium emission line is located. Comparing the amount of light coming through that filter with the amount coming through a broader filter around that area could tell us if the object has helium emission or not. This way, we could search for AM CVns a lot more efficiently, since photometric observations can be done and analyzed a lot faster than spectroscopic ones.

Using the tactic outlined in the above paragraph, a survey was done of 40 square degrees of sky at a Galactic latitude of 15 degrees. The core of the Galaxy is situated at 0 degrees latitude, so at 15 degrees we are looking at a section slightly above or below the disc of the Galaxy. This was done because you expect more stars towards the disc of the Galaxy and observations with too many stars are difficult to analyze. So, the aim is to look not directly at the centre, but also not too far away from it. The survey was split in two parts, one part observed from the northern hemisphere with the KPNO Mosaic I instrument and the other part observed from the southern hemisphere with the ESO 2.2m Max Planck telescope in La Silla, Chile, using the WFI (Wide Field Imager) instrument. The latter part is the object of this thesis, since this data was already embedded in the Astro-WISE system (see the next chapter for more information on this). The survey was done from the 18th to the 24th of July 2001. The 18 square degrees of the survey observed with the ESO 2.2m WFI camera were divided among 29 fields.

The WFI camera consists of 8 distinct CCDs (for more information about the CCD and its workings, see the next chapter). The images were taken in four filters: a blue filter, a red filter, a narrow helium filter (centered on the 667,8 nm helium emission line) and a narrow H-alpha filter (H-alpha is one of the primary hydrogen emission lines at 656.3 nm, close to the 667,8 nm helium emission line). The blue and red filters can give us the colour and the relative brightness of each source found in the survey. The brightness of the object in the helium filter, when compared to the brightness in the red filter, can tell us if the object has helium emission. This can thus narrow down interesting candidates for an AM CVn search. However, if the spectrum has certain slopes of the continuum the helium characteristic may be unclear when looked for with this method. As an extra search option, we can compare the brightness

in the helium filter with that in the H-alpha filter. If the object is far brighter in the helium filter, we may be looking at an AM CVn. Figure 2.5 shows the fraction of light the filters let pass at each wavelength. Also shown in this figure is the spectrum of an AM CVn (J1208). As can be seen, the object is brighter in the blue area of the spectrum and the helium filter clearly picks up the helium emission.

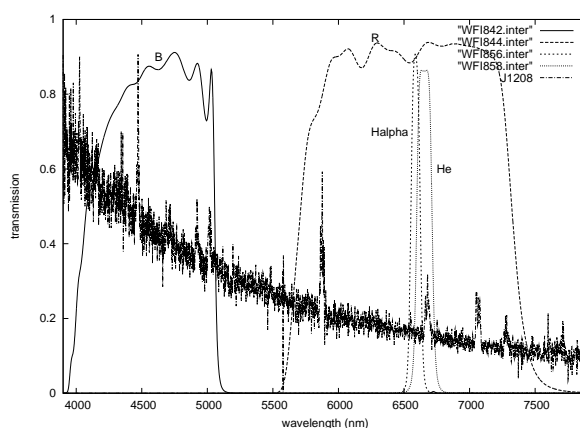


Figure 2.5. Filter response curves overlaid on the spectrum of an AM CVn (J1208). The y-axis shows the fraction of light the filters let through. The x-axis shows the wavelength of the radiation. It can be clearly seen that the helium emission is picked up specifically by the helium filter.

The amount of data from this survey, although it is not a very large one, is still extensive. It thus must be analyzed in an orderly, comprehensive way. There are software packages that can assist an astronomer with a job like this one. One of those packages is called "Astro-WISE", and this is the one we opted to use for this research. In the next chapter, we will explain what Astro-WISE is and how we have used it to analyze the AM CVn survey.

Chapter 3

Astro-WISE

In this chapter we will describe the aspects of the Astro-WISE system and give an overview of how it has been used to analyse the data from the AM CVn survey (as described in the previous chapter) between september 2007 and august 2008. We will start with a short overview of the path a photon (light particle) traverses from a source to our detectors, in order to better explain why all the different steps in the Astro-WISE analysis routine are needed. Then we will give some general information about Astro-WISE, before going into detail about the steps required to turn raw data into an image we can use. Finally, the endresult of the Astro-WISE system as used in this research will be described, and the system as a whole will be evaluated.

3.1 The path of a photon

A source on the sky (which will generally be a single or binary star in our case) sends out light (actually all sorts of electromagnetic radiation) in the form of photons. These photons travel in all directions, including our direction. Sometimes they go through dust clouds, which reddens and partly extinguishes the photon stream. Eventually the photons will hit our atmosphere. Our atmosphere can distort the photon stream since it is turbulent and full of molecules. The longer the photons have to travel through the atmosphere before they reach our detector, the more the stream will be distorted. In practice this means that looking straight up, one will catch less distorted photon streams than looking more towards the horizon. As if this were not enough, our atmosphere also changes continuously.

Once the photons have finally hit our telescope, they go through a series of lenses and mirrors to focus them onto the endpoint: a detector. In our case this detector is a CCD camera. A CCD (Charge Coupled Device) camera consists of many small areas called pixels. A photon striking such a pixel will free an electron. This electron will be counted when the CCD is read out. In this way, one can learn how many photons have struck. Of course, the system is not perfect. Certain pixels can have freed electrons due to heat effects. A pixel may also be not exactly as sensitive as the other pixels. To correct this, we take several "pictures" of black or constant backgrounds. These will all be explained later in this chapter, in section 3.4.

Finally we will end up with a count of the electrons in each pixel, combined in a so-called "frame". This is the raw data, the unaltered "photograph" we have to work with. This is where the Astro-WISE system comes in. The system will convert this raw data to data we can use for scientific analysis, which is the goal of this so-called data reduction. This conversion process is divided into the following steps: making

a Bias and Flatfield frame, Reducing the image, creating Astrometric and Photometric parameters, Re-gridding the image, creating a Sourcelist, creating an Associate List and finally exporting the data from the system in a form we can use. This entire process is explained in detail in section 3.4. We will now first give some general information on the Astro-WISE system.

3.2 What is Astro-WISE?

Astro-WISE stands for Astronomical Wide-field Imaging System for Europe. It is an information system, which means that it has been developed to handle (astronomical) data with the goal of exploiting this data scientifically. It is set up to incorporate all the steps from the archiving of the raw data, via the calibration and analysis of this data, to the archiving of the results. Basically this means that you put your raw data into Astro-WISE, which leads (via several user-initiated steps) to results that can be retrieved, published and/or archived. For this research these results were in the form of lists of sources in the AM CVn survey with the brightness of these sources in all four filters. This brightness is in astronomy given in so-called 'magnitudes', which is basically a logarithmic unit of brightness that *decreases* when the brightness of an object *increases*.

The Astro-WISE system was designed specifically to handle the huge amounts of data involved in modern-day scientific research. In contrast to some older systems, Astro-WISE allows the user to retrace all the steps used in making an end-product back to the original raw data. This comes in very handy when one is not satisfied with the endresult and would like to change one certain thing in the analysis process and remake the product. Also, data that has been made public can be viewed by anyone, and people with an account for the Astro-WISE database can use it to make their own products. This of course makes it very easy to work on a project with multiple people, or for instance check how data analysis was done on an older project.

These characteristics make Astro-WISE a promising candidate for the future of astronomical analysis in Nijmegen. We've used Astro-WISE on the AM CVn survey to test the features of the system and gain familiarity with it, which should enable us to advise others at the Radboud University about its use.

In the next section we will explain in detail the different steps required to come to our end-product, as outlined in section 3.1. In sequence these will be: Bias, Flatfield, Reduction, Astrometric and Photometric Parameters, Re-gridding, Sourcelist and Associatelist and finally the exporting job. Each part will be accompanied by comments about the Astro-WISE system and we will end with a short evaluation of said system.

3.3 The Target Processor

Normally one would start a job with Astro-WISE by ingesting the raw data into the database. In this case however, all the data was already present in the Astro-WISE system. Thus we could immediately start with the calibration and analysis of this raw data. Astro-WISE basically has two ways to interface with the system. One is a command prompt, where users can query for data and perform actions on this data. Astro-WISE uses the programming language Python, which in practice means that queries and scripts can be entered in this language on the command prompt. The second way of interfacing with the system is a series of graphical web-tools. In general, the web-tools give a better overview of the data and are easier to master. However, the command prompt has more options and allows the user to tweak almost every aspect of the data calibration and analysis. For this research we used both the command

prompt and certain web-tools, depending on what exactly we wanted to accomplish.

With the raw data ingested in the system the next goal would be to derive so-called "Regridded Frames". These are images that are corrected for any distortions and are astrometrically and photometrically calibrated. Astrometric calibration means the exact position of the image on the sky is checked. Photometric calibration means the brightness of the stars on the image is compared to the brightness of certain 'standard stars' to remove any atmospheric dimming effects. All this is done in a number of steps. We used the "target processor" webtool of the Astro-WISE system for this, not the command prompt. The reason for this choice is that the target processor gives a comprehensive overview of all your data, processed and unprocessed, and is faster when processing a small number of images analogously. For large bulks of images, the command prompt would be more suited.

When starting up the target processor, one will see the screen as shown in Figure 3.1. On the left side menu, you can login and select a project and instrument. Then, on the middle of the page, you can select a 'target'. The target is what you want to make, for example a Reduced Science Frame or a Master Bias Frame. The targets relevant to this research will be explained later in this section. For the others we refer the reader to the Astro-WISE manual.

The screenshot shows the Astro-WISE Target Processor interface. On the left is a navigation menu with sections: Astro-WISE Homepage, Target Processor TEST VERSION, Contact (Willem-Jan Vriend), DB User (awospooren), Help (Getting Started), Project (WFI@2.2m), Instrument (WFI), State (1. Preselect Target, 2. Specify Target, 3. Select Target(s), 4. Process or Query), and Options (Preferences, Process Parameters, Upload Code, Job overview). The main content area is titled "Select target for WFI" and includes instructions: "Select the target for processing. On the left are the image pipeline targets, on the right the calibration." Below this are two columns of target options:

- Image pipeline targets:
 - ReducedScience
 - RegridDEDFrame
 - CoAddedFrame
 - SourceList
 - AssociateList
 - GalPhotModel
 - GalFitModel
- Calibration targets:
 - Astrometric
 - ColdPixel
 - DomeFlat
 - Fringe
 - HotPixel
 - MasterBias
 - MasterFlat
 - Photometric
 - PhotSrcCat
 - ReadNoise
 - TwilightFlat

At the bottom, there is a footer with page generation information: "page generated 2009-09-01 15:22:55.537625", "generation time 0:00:00.100680", and "For optimal experience use firefox browser". To the right of this is the text "empowered by" above the Astro-WISE logo.

Figure 3.1. The opening (preselect target) screen of the Astro-WISE target processor. Here you can select the type of action you would like to perform.

Once the user has selected a target, the next screen, as shown in Figure 3.2 will pop up. Here you can select a period to search in the database, as well as limiting the search to a specific filter. When you click 'Show', The top of the screen will show the data available in the database. The data is shown in blocks, each block representing all observations done in a certain filter on one specific night. Hovering over a block with the mouse cursor will give you more information on the block. Clicking on a block brings up the next screen.

Figure 3.2. The specify target screen of the Astro-WISE target processor. Here you can select the specific block of data you would like to query or perform an action on.

After selecting a block of data on which you would like to perform an action, the screen as shown in Figure 3.3 will appear. Here you can select the specific image(s) on which you would like to perform the action. Subsequently clicking 'Process' will perform the action selected in the first screen (the 'target'), leading to the screen shown in Figure 3.4. Here you can set many parameters concerning the processing job (we refer to the Astro-WISE manual for a more detailed explanation of all these) and submit it to a computing cluster which will perform the job. Clicking 'Query' in the screen shown in Figure 3.3 will bring up the screen shown in Figure 3.5. This will show you what elements have been used to create the object you selected, or which elements will be used in its creation if it hasn't been created yet. This is the way the target processor works in general, in the next section we will describe exactly what we did in more detail.

Astro-WISE
Homepage

Target Processor
TEST VERSION

Contact
Willem-Jan Vriend

DB User
awospooren

Help
Getting Started

Project
WFI@2.2m

Instrument
WFI

State

- Preselect Target
- Specify Target
- Select Target(s)**
- Process or Query

Options

- Preferences
- Process Parameters
- Upload Code
- Job overview

ReducedScienceFrame (RawScienceFrame)

Select which ReducedScienceFrame target(s) to process or query. When querying, the query depth ca

- Click on a ccd link to view the frame, if the ccd is printed bold the corresponding object has been

Query Depth :

	<input type="checkbox"/>	Observation	Filter	Observer	Object	Observing Block	Processed
1	<input type="checkbox"/>	23 Jul 2001 23:51:23	#842 JohnsonB	UNKNOWN	ames26	-1	ReducedScienceFra
2	<input type="checkbox"/>	24 Jul 2001 00:29:20	#842 JohnsonB	UNKNOWN	ames27	-1	ReducedScienceFra
3	<input type="checkbox"/>	24 Jul 2001 01:19:10	#842 JohnsonB	UNKNOWN	ames28	-1	ReducedScienceFra
4	<input type="checkbox"/>	24 Jul 2001 02:13:55	#842 JohnsonB	UNKNOWN	ames29	-1	ReducedScienceFra
5	<input type="checkbox"/>	24 Jul 2001 03:06:43	#842 JohnsonB	UNKNOWN	ames31	-1	ReducedScienceFra
6	<input type="checkbox"/>	24 Jul 2001 03:52:50	#842 JohnsonB	UNKNOWN	ames32	-1	ReducedScienceFra
7	<input type="checkbox"/>	24 Jul 2001 04:32:28	#842 JohnsonB	UNKNOWN	ames33	-1	ReducedScienceFra
8	<input type="checkbox"/>	24 Jul 2001 04:50:48	#842 JohnsonB	UNKNOWN	KS1 731-26	-1	ReducedScienceFra
9	<input type="checkbox"/>	24 Jul 2001 05:02:16	#842 JohnsonB	UNKNOWN	SA1 10-355A	-1	ReducedScienceFra

or

page generated 2009-09-01 15:25:26.296683
generation time 0:00:00.229091
For optimal experience use firefox browser

empowered by


Figure 3.3. The select target screen of the Astro-WISE target processor. Here you can select the specific image from the observing block previously selected to query or process.

3.4 From raw data to image

We first started to create a Master Bias Frame. A Bias Frame is basically an image taken 'with the cap still on the camera', so of an entirely black field. This is done to determine the value pixels give without a light source, so we can later correct for this 'bias'. When an astronomer makes this image, it is tagged as being a Bias Frame. Usually multiple bias images are taken for each observation night (or for a few nights), since coincidental extremities can occur in one single image. Astro-WISE averages out these images, combining them into one frame, called the Master Bias Frame. This Master Bias Frame is then used to correct the observational data. A simple click on "MasterBias" as target (see Figure 3.1), then selecting the bias images you want to use from the database (Figure 3.2) and two more clicks on "Process" and "Submit" (Figures 3.3 and 3.4) suffices to create the Master Bias Frame with the target processor.

The next step is to create a Master Flatfield Frame. A flatfield is an image taken of a more or less uniform surface, such as the dome of the telescope or the twilight sky (both of these can also be made and combined). An image like this can show the observer the sensitivity of the different pixels, as well as point out any dead ("cold") pixels on the CCD camera. Since the surface imaged is uniform, each

Homepage

Target Processor
TEST VERSION

Contact
Willem-Jan Vriend

DB User
awospooren

Help
Getting Started

Project
WFI@2.2m

Instrument
WFI

State
1. Preselect Target
2. Specify Target
3. Select Target(s)
4. Process or Query

Options
Preferences
Process Parameters
Upload Code
Job overview

Job Submit

The following table gives an overview of what is going to be processed. The help pages for this fo

Option	Value
Target	ReducedScienceFrame
Date	23 Jul 2001 23:51:23 - 24 Jul 2001 05:02:16 (72)
Instrument	WFI
Filter	#842
Chips	ccd50,ccd51,ccd52,ccd53,ccd54,ccd55,ccd56,ccd57

The following DPU's will be used, for the specified user, project and context. You can override the

Option	Value
Single Host	dpu.hpc.rug.astro-wise.org
Parallel Host	dpu.hpc.rug.astro-wise.org
Processing depth	1
Custom code	No
User	awospooren
Project	WFI@2.2m
Privileges	1

The following DPU options are available. They specify how many and which nodes will be used. A available for all targets, these are greyed out.

Options	
<input checked="" type="radio"/>	Group jobs per chip on a node
<input type="radio"/>	Maximize nr of jobs
<input type="radio"/>	Specify number of nodes to use <input type="text" value="72"/>
<input type="checkbox"/>	Force the short queue
<input type="checkbox"/>	Global Astrometry (GAS)
<input type="checkbox"/>	Run GAS on single host
<input type="checkbox"/>	Reserve all nodes at once (for synchronous jobs)

Submit

Figure 3.4. The process screen of the Astro-WISE target processor. Here you can set many parameters concerning the processing job and submit it to the computing cluster that will perform the job.

pixel should give the same value. Because their sensitivities differ however, they do not. The flatfield works thus as a sort of map of the sensitivity of the different pixels, and any pixel not responding at all (the cold pixels) is clearly shown. An image like that is tagged as a "Dome Flat Frame" or "Twilight Flat Frame" when made. With Astro-WISE's target processor, one can first correct all the flatfields for the bias using the Master Bias Frame previously created (select "Dome Flat Frame" and "Twilight Flat Frame" as target, select the flatfield images and click "Process", analogously to the Master Bias Frame) and then proceed to create a Master Flatfield Frame from these images. Again this uses the "select target, select source, click process"-way. With this Master Flatfield Frame as source, one can also create a so-called Cold Pixel Map, which as the name says is a map of all the cold (dead) pixels on the CCD which can be used to filter these pixels out of the observations.

With a Master Bias Frame and a Master Flatfield Frame for a certain observation night in hand, the raw data of that night can be 'reduced'. This means it can be corrected for the bias, cold pixels and

Figure 3.5. The query screen of the Astro-WISE target processor. Here you can see what elements have been used to create the specific bit of data you selected previously, and if needed process it further.

the sensitivity of the different pixels, so that only the light from the actual celestial sources remains. This is done in three steps. First by subtracting the Master Bias Frame from the image in question to remove the values the pixels give due to heat effects. Then flagging the cold pixels so they are not used in any calculations and finally dividing the value each pixel gives by the value it gives in the Master Flatfield Frame to correct for their relative sensitivity. With the target processor it is again a simple and straightforward job to select Reduced Science Frame as target, select the images that you want reduced and then process them. The most recent Master Bias Frame and Master Flatfield Frame valid for that observation night are automatically selected. There is another webtool that allows you to check and change exactly which frames are used in the reduction process, should you not concur with the automatic selection. This tool is called "calts". We will not go into detail about it here.

One might think that with the Reduced Science Frame we have obtained a "true" image of the sky. However, such frames still suffer from distortions (mainly resulting from the optics of the telescope) and thus uncertainties in the positions of the sources. To correct this we select the Astro-Wise target "Astrometric

Parameters” and as source we use the Reduced Science Frame we just produced. Basically this compares the positions of the best measured sources in the Reduced Science Frame with the positions of these sources in a standard catalog. This information is used to provide a set of parameters with which the image can be rotated and transformed to remove the distortions and better resemble the true look of the sky.

Now we have arrived at the final correction to the raw science data. Due to changes in the atmosphere from night to night and the change in the pathlength of the photons through the atmosphere, stars do not appear at the same brightness during the entire night and between nights. To correct this, astronomers take an image of a so-called ”standard star field”, in which there are stars of which we know the inherent brightness (for example via long subsequent observations, via space observations, or by observing the star when it is directly above you with excellent atmospheric conditions). The known brightness is then compared to the brightness in the image of that night, which allows us to then correct all images of that night for this offset. With the target processor of the Astro-Wise system this is done by selecting the target ”Photometric Parameters” and subsequently selecting the standard star field that is to be used. This creates a set of parameters to correct the brightness offset for all images of that night. A small sidenote here: in addition to the blue and red filters of the AMCVn survey, Helium and H-alpha filters were also used. Since there are no standard star values in the Helium and H-alpha filters known, the photometric correction is not available for these filters. This has as a consequence that the brightness of the sources in these two filters can only be viewed relatively to other sources on the same frame and not absolutely or relative to other frames.

The Astrometric and Photometric Parameters still have to be used on the Reduced Science Frame to create the endresult: the Regridded Frame. Simply select the target ”Regridded Frame”, choose the Reduced Science Frame to regrid and the system searches for the parameters available automatically. This leaves us with true images of the sky that can now be analyzed to gain scientific information from them.

To check the quality of the obtained images, you select Regridded Frame as target in the Target Processor, but subsequently choose ”query” instead of process (in Figure 3.3). This will give you a tree with all the dependencies of the Regridded image (so you see what has been used to make it) like in Figure 3.5. Each of these endresult and source images can then be viewed with one mouseclick, allowing you to check for artifacts or other discrepancies. In our experience the quality of the gained images is not as good as it could be, yet as explained later there is another step in our analysis that removes most remaining faults. Since we have no experience with other image reduction software packages, we cannot compare the quality of Astro-WISE to them. This is left up to the reader.

3.5 Lists and evaluation

As explained in section 2.5, we need the brightness (magnitude) of all four different filters for all objects to search for AM CVns. So what we want from the images is a list of all sources with their magnitudes in the four different filters. The method to do this in Astro-Wise is to create a SourceList, which is a list for an image (in one filter) of the properties we require (and many more) . This is where we leave the Target Processor webtool of Astro-Wise and use the command prompt instead. The Target Processor is not versatile enough at this point to create what we want. It can only create SourceLists from Co-Added Regridded Frames, a type of image that has added all the images of the chips (of which there are eight) on the CCD camera together into one big image. However, since the images we have in the Helium and H-alpha filters are not Regridded Frames but Reduced Science Frames (since we couldn’t determine the Photometric Parameters), the Target Processor’s way of obtaining SourceLists is not useful for us.

Astro-WISE makes SourceLists by basically going over each image and noting any area of pixels that has a significantly higher value than 0 (a source). Thanks to the Astrometric Parameters described in the last section, the coordinates of the source are known. And thanks to the Photometric Parameters the actual brightness (magnitude) on the sky of the object can be deduced (by comparing them to the brightness of standard stars in the survey). The coordinates and these magnitudes are what we need.

Making SourceLists (or any object for that matter) with the command prompt is slightly more complicated than using the Target Processor. It requires a sequence of commands to be entered. Basically you first query for the objects you want to create sourcelists for in the database (see the Astro-WISE How-to on querying for more information on this). Once you have these objects "selected" (assigned to a certain variable) you can perform the necessary commands on them. In the appendix is a script we used to create all sourcelists needed from the queried frames in one go. Be advised that it takes the Astro-WISE system some time to process all these commands. Also, the script to create the sourcelists from Reduced Science Frames (for the Helium and H-alpha filters) is slightly different from the one used to create sourcelists from Regrided Frames (for the Blue and Red filters). It may seem to the reader now that using the command prompt is not that difficult at all, but be advised that it takes some time to familiarize yourself with the Python Programming language and the commands as given in the Astro-WISE How-To before one is able to create the scripts needed to do things efficiently.

Now that we have lists with the positions and magnitudes of the sources in the four different filters, we would like to compare these lists with each other. Each source in each filter needs to be associated with the same source in another filter, so that we end up with a list of sources and their magnitudes in all filters instead of a list of sources for each filter separately. Luckily Astro-WISE incorporates an object like this, called an Associate List. When creating this object, one picks two sourcelists. For each source in one sourcelist, it searches for another source within a certain small (user-defined) distance (on the sky) in the other sourcelist. When it finds one, it considers these sources the same and 'associates' them, meaning they are put in the Associate List together. Once the Associate List is complete, other sourcelists can easily be added to it via the same process. The script to do this all in one go for a query of sourcelists can be found in the appendix. Do note that this script is for the blue, red, Helium and H-alpha filters of the WFI telescope. For different filters, simply change the filter.name parameter.

A short intermezzo about database errors here might be in order. There were apparently (we're no experts by any means) some errors in the Oracle database system used by Astro-WISE. One of these made it impossible to run too long scripts for extended periods of time. The Associate List script was unfortunately one of those scripts. This means that after about half an hour (that was for our user account, apparently it could differ between accounts) an error was produced and the calculation was cancelled. So to create a lot of Associate Lists, we had to split the work up in segments. We tried to shorten the script, to no effect. Luckily this particular error is solved in the current version of Astro-WISE. Whilst on the subject of database errors, it might also be worthwhile to note that idling too long on the command prompt can cause Astro-WISE to 'hang' on the next large command. A simple reboot of Astro-WISE solves this issue.

One might wonder about the quality of the SourceLists and AssociateLists. To check this, one would want to overlay the found sources (pictured by circles for example) on the images, to check whether they correspond to actual light sources. With Astro-WISE you can use the `make_skycat` method (see appendix) to create a so-called 'skycat catalog' for a certain Source or Associate List. With the program 'skycat' (or its expanded version 'gaia', which is used in Nijmegen) it is then possible to load this catalog on top of an image, creating exactly the overlay we want to see. When we first used this method on a SourceList, the amount of erroneous sources found was larger than we expected. Very bright stars tended to create multiple sources, certain artifacts left in the image were identified as a light source (while they

obviously were not), faint stretched sources would be seen as multiple sources and on the edge of the image mistakes would occur due to the sudden cutoff. No reason to panic here though, since these results are not filtered yet. The program incorporated into Astro-WISE that is used to extract the sources from an image (SExtractor) recognizes many possible faulty sources and flags them. This is done by using a so-called 'weight-map', which gives a value to each pixel that reflects the quality of that pixel. When associating the Source Lists into an Associate List, the flagged sources are omitted. So, when we subsequently used the `make_skycat` method on an Associate List, it became apparent that almost all mistakes had been removed. One should note that several 'good' sources were removed as well, but since these were a very small percentage (2-3%) and mostly very bright sources this was deemed unimportant for this research (since AM CVns are expected to be faint). A final remark on this: the SExtractor program has many options that can be edited by the Astro-WISE user, such as when exactly to flag a source as faulty. See the Astro-WISE how-to and the SExtractor manual (googleable) for this.

The Associate Lists we obtained can be used to make colour-colour diagrams of the stars in the field. A colour in astronomy is usually defined as the magnitude in one filter subtracted by the magnitude in another filter, since this shows how bright the source is in one side of the spectrum compared to another. A colour-colour diagram is a plot of two different types of these colours against each other, for example by subtracting the red magnitude from the blue magnitude and plotting this against the Helium magnitude minus the red magnitude. This gives us more information about the type of star we're dealing with and helps to identify potential AM CVn candidates (see the AM CVn chapter for more information on this). It is possible to use Astro-WISE to plot these diagrams, as it has an integrated plot program (called `pylab`). However, we chose to use our own plotting programs in Nijmegen. Thus, we had to export the Associate Lists from the Astro-WISE database to the drives in Nijmegen. This is unfortunately not as straightforward as it seems. One could use the "DBview" (Database viewer) webtool for this. However, this tool is aimed towards viewing single database objects. This means that to export all Associate Lists one would have to do this one by one manually, which is cumbersome. Instead we decided to write another script. It can be found in the Appendix. It writes the queried Associate Lists to the current directory. It selects certain data from the Associate Lists, we chose (in the end) the coordinates of the source, its magnitude, the error on this magnitude and an ID specific to the source.

At this point we have reached the end of the Astro-WISE portion of this research. All in all we are pretty satisfied with the system. We were able to complete the data reduction and analysis in a relatively short amount of time, even though we ran into some problems on the road. It takes some time to familiarize yourself with the system. Also, it's obvious that while the Astro-WISE reduction pipeline is in working order, improvements can still be made (and are being made). We ran into several bugs (some caused by changes in the design while we were working) yet the team in Groningen was always willing and almost always able to help me. Several new features have been introduced at my request, such as a `make_skycat` method for Associate Lists. The installation in Nijmegen also took some time, but is definitely an improvement over using an SSH session to Groningen. We are confident at this point that a new user in Nijmegen will not experience most of the problems that we did, and will see a fast and mostly effortless data reduction and analysis process.

Chapter 4

Analysis

This chapter will reveal how the data exported from the Astro-WISE system was further analyzed. We want to take the data in the form of SourceLists and AssociateLists that we gained in the last chapter and modify it in such a way that we can find AM CVns in it within a reasonable timeframe. So the chapter starts off with a description of the data. It then continues with the way it was altered to suit our specific needs (mostly via a median correction). Then it explains how we made colour-colour diagrams, including a theoretical main sequence and the AM CVns already known. The colour-colour diagrams are the tools we use to look for AM CVns, a process explained in the next chapter. In conclusion, this chapter also explains why we disregarded some of the observation fields.

4.1 The Data

As made clear in the Astro-WISE section of this thesis, we exported Associate Lists from the Astro-WISE system for further examination. These Associate Lists contain four rows for each source, with in each row columns for its coordinates, magnitude, error on the magnitude and its ID. There are four rows because the magnitude is given in four filters (the Johnson-B, Cousins-R, Helium and Halpha). In each of these four rows the coordinates are (almost) the same, as is the ID specific to the source. As Associate Lists are specific to each CCD, we have eight lists per field.

From the data in the above described form, we wish to distill possible AM CVn candidates. We know that AM CVn systems are blue systems that have Helium emission. So we should look both at the colour of the sources in our data (which means the value of the B magnitude compared to the R magnitude) and the brightness of the source in the Helium filter compared to its brightness in the R and Halpha filters (the latter because it is a good indication of the continuum brightness of the star near the Helium filter). We figured that the most efficient way to do this is to produce colour-colour diagrams of the observed fields and look for outliers in the area where we expect AM CVns to lie. A colour-colour diagram is a plot of the magnitude of the source in one filter minus its magnitude in another filter, versus the same thing for one or two different filters. Since the magnitude scale is a logarithmic one, the magnitude of A minus the magnitude of B simply equals the flux of A divided by the flux of B. This means that the result is independent of distance, brightness of the source, etc. If we would be able to predict in a colour-colour diagram where the main sequence stars should lie, and plot where the currently known AMCVn's are located in this diagram, we would know where to look for more AM CVns in the sample.

We decided to make four different colour-colour (actually one of them is a colour-magnitude) diagrams

for each field, the combination of which should enable us to isolate the interesting sources. These four are: He-Ha versus B-R, He-R versus B-R, Ha-R versus B-R and He-Ha versus B. The He-Ha versus B-R and He-R versus B-R are important to identify possible AM CVns, since they show whether the object is blue and has possible Helium emission. The Ha-R versus B-R shows whether there are peculiarities with the H α emission/absorption of the source, which may make the He-Ha value unreliable. The He-Ha versus B diagram allows us to identify interesting sources, since bright sources are likely to have little peculiarities in their He-Ha unless they are a special (non-main sequence) object. This is because bright main sequence objects usually have no significant Helium and H α absorption/emission, so their He-Ha value should be around 0.

The first step in making the desired colour-colour diagrams was to extract the necessary data from the Associate Lists into a form that could be used to make the plots we desired. To accomplish this a C++ program was created that made lists of the B-magnitude, its error, the other magnitudes and their errors and finally the IDs, each in a separate file, for each Associate List. Using the simple Unix commands 'awk' and 'paste', these files could subsequently be combined, the different magnitudes substracted from each other, the errors added up quadratically and the IDs linked to the correct source. Scripted, this can relatively quickly make files that feature for example a column with He-Ha, a column with B-R, a column with the He-Ha error, a column with the B-R error and a column with the source IDs. Using gnuplot, it is then straightforward to make a He-Ha versus B-R plot, which is in fact our colour-colour diagram (see for example Figure 4.3).

4.2 Median correction

One CCD of a field usually features a couple of hundred stars in this survey. After viewing a few plots, we deemed it more efficient to combine the eight CCDs of each field into one, to get a couple of thousand stars in one diagram. There would still be sufficiently few outliers to be able to identify them easily, and it would take considerably less time. To combine the data files of each CCD into one data file for the entire field, the 'awk' command was once again used.

As one might remember from the Astro-WISE chapter of this thesis, the Helium and H α filters could not be photometrically calibrated. This gives us rather strange values for He-R and such. He-R for example should be around 0 when the object has no Helium emission or absorption, but because R is photometrically calibrated and He is not, the result is a rather large negative value instead of one close to 0. In principle we do not need the Helium and H α filters to be photometrically calibrated, since we can still compare sources to others in the same field, which is enough to find peculiar sources like AM CVns. All we need to do is recognize the main sequence in our colour-colour diagrams and compare this to a theoretical main sequence. The main sequence (see chapter 2) is the line in a colour-colour diagram where by far the most stars can be found. Stars with peculiar Helium or H α (like AM CVNs) stand out. The AM CVns already known can be placed in relation to a theoretical main sequence. Overlaying this theoretical main sequence on the main sequence actually found in our diagrams allows us to place the known AM CVns in our plots. This then allows us to find interesting candidates by searching in the area where these known AM CVns are located. To make this more easy, we decided to shift He-Ha, He-R and Ha-R such that they are centered around zero. We did this by calculating the median of the He-R, Ha-R and He-Ha magnitudes of the sources for each field, and substracting these values from He-R, Ha-R and He-Ha, thus creating new values around zero.

After substracting the median in the fashion outlined above, we noted that not all fields had their distribution centered around zero as well as we would like. Looking for the cause of this problem, it became

apparent that in the He-Ha versus B graphs of many fields, the "tail" of the sample (the fainter sources with higher B magnitudes) curved off towards the left or right. See for example Figure 4.1. We will come back to this odd behaviour in section 4.4. For now, we surmised that leaving the sources with higher B magnitudes out of the median calculation would solve the issue. After trying several different values for the cutoff, sources with B magnitudes higher than 20 were not included in the sample used to calculate the median. We also tried calculating the median for each CCD, and correcting the He-R, Ha-R and He-Ha values, separately before combining the CCDs into an entire field. This offered a better result, with the sources more strongly clustered around zero, so this approach was chosen over the previous method.

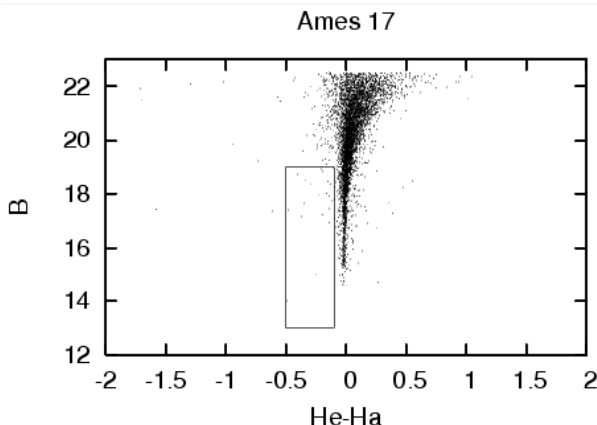


Figure 4.1. He-Ha versus B plot of field Ames 17. Note the 'tail' of the source distribution curving off to the right. The box will be explained later in this thesis.

4.3 Theoretical Main Sequence and known AMCVn's

As said before, if we can put the known AMCVn's in our colour-colour diagrams, we know where to look for new ones. However, since we haven't absolutely calibrated all magnitudes, we can't just look up the magnitudes of the known AMCVn's and plot them in the diagram. There is a workaround for this problem though. Since we know the position of the AMCVn's relative to the main sequence, and we know the main sequence is always the same, we could simply overlay a theoretical main sequence on our data and plot the known AMCVn's relative to that. When we do this we have to account for two things. First is the fact that we shifted to positions of our stars in He and Ha in order to align them on zero. We should do the same for the theoretical main sequence. Second is that our sources will be reddened due to the dust between us and them. The Galaxy contains a lot of dust, and since we are looking at a position on the sky close to the disc of the Galaxy, we are looking through some of it. The dust scatters the photons, which makes them lose energy and thus become redder. We can obtain the reddening factor with the NASA/IPAC Galactic Extinction Calculator (<http://nedwww.ipac.caltech.edu/forms/calculator.html>). It turned out that for our fields the reddening factor is about 0.5.

The theoretical main sequence for reddening factor 0.5 and the positions of the AMCVn's relative to this were kindly provided by K. Verbeek (see also Verbeek et al. (2008)). We calculated the median for this in the same way we did for our own data and shifted it accordingly. We then plotted this main sequence in our colour-colour diagrams, along with the positions of the known AMCVn's. An example of this for

a Ha-R versus B-R diagram can be seen in Figure 4.2.

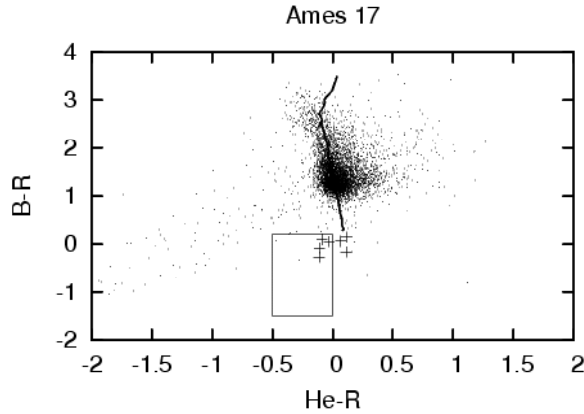


Figure 4.2. He-R versus B-R plot of field Ames 17. The thick line is the theoretical main sequence, the crosses are the positions of known AMCVn's. The box will be explained later in this thesis.

For the most part, the line of the theoretical main sequence matches the positions of the bulk of the stars in our sample well. However, as can be seen in Figure 4.2, for large B-R the sequence of stars bends the other way than the line of the theoretical main sequence. We do not know why this occurs, but it may be related to the "tail" phenomenon mentioned before (which will be further examined in section 4.4). Since this only occurs for large B-R, in the area where red stars lie, this is not important for our AM CVn search since AM CVns are blue objects. In light of this, we continued to search for new AM CVn candidates around the positions of the known AM CVns in our diagrams. We will describe this search in the next chapter.

4.4 Bad fields

As mentioned above, many fields have a 'tail' that curves off either to the left or to the right at higher magnitudes. We have no idea what causes this behaviour. No link could be found between the objects thus affected and for example their position on the CCD. In view of the time, we decided to simply disregard those fields that were affected so much that we no longer found a search for AMCVn's in these fields feasible. Examples can be found in Figures 4.3 and 4.4. Of the 29 fields we have in total, 6 fields were deemed 'bad'.

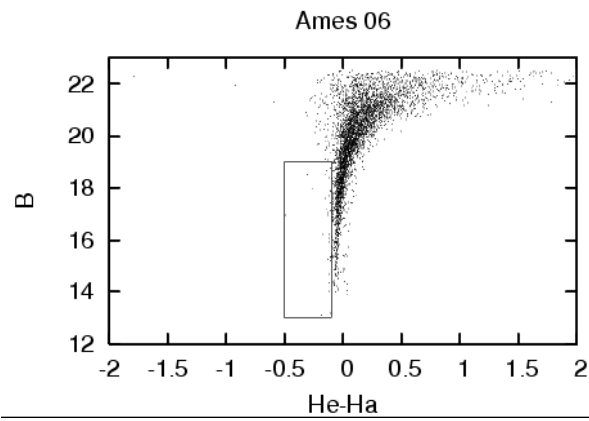


Figure 4.3. He-Ha versus B plot of field Ames 06. As can be seen, the curvature of the tail is so severe that it affects the entire sample. The box will be explained later in this thesis.

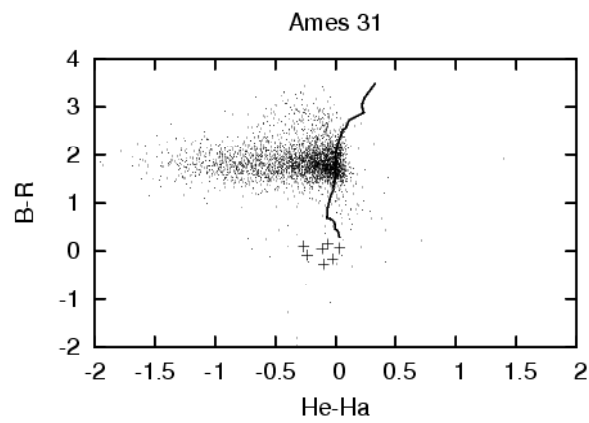


Figure 4.4. He-Ha versus B-R plot of field Ames 31. The curve of the tail shows itself in other diagrams too, displacing many sources far from the main sequence.

Chapter 5

Results

In this chapter we will explain how we went about our search for new AMCVn's and other interesting objects. First we show what objects we selected from the data, why we selected these particular objects and in what categories they fall. Then we will show the amounts of objects found in each category.

5.1 Selection Boxes

As the first step in the search for AMCVn's, we created two selection boxes that should contain most of the potentially interesting objects. These boxes can be seen in Figure 5.1. Objects without helium emission should have He-R around zero, since the area where the helium line would appear lies in the middle of the red area of the spectrum. So without helium emission, the brightness in the helium filter should be equal to the brightness in the red filter. This suggests that objects *with* helium emission can be found in the He-R < 0 area. The box in the He-R versus B-R diagram was chosen such to contain blue objects with Helium emission as well as half of the known AM CVns. We did not extend it further to the right because while that area contains known AM CVns, it is also so close to the main sequence that objects found there would not likely be AM CVns. We realise that we lose potential candidates in this way, but it does make the candidates we do find more likely to actually be AM CVns. We did extend it quite far to the left since there lie the objects with more pronounced Helium emission. We used the He-R versus B-R diagram instead of for example the He-Ha versus B-R diagram because there are less other (non-AM CVn) sources around the known AM CVns in the He-R versus B-R diagram. The box in the He-Ha versus B diagram was chosen such to include objects bright in the blue with Helium emission or H-alpha absorption, so this is likely to contain AM CVns.

A C++-program was written to select the objects in the boxes from the data. They could then subsequently be plotted in the colour-colour diagrams. See for instance Figure 5.2. Of course, not all objects in the boxes are equally likely to be AM CVns. So we imposed additional criteria on the selection and created four different categories in which to divide the interesting objects.

The first category, category A, contains all objects residing in the box in the He-R versus B-R diagram that also have He-Ha smaller than zero. These objects are blue and are very likely to have Helium emission features, giving them a very good chance to be AM CVns. This category contains the objects most interesting to us. Category B includes those objects that are located inside the box in the He-Ha versus B diagram and also have He-R between -0.5 and zero. These are once again objects likely to have Helium emission, and are also relatively bright in blue. While it is less likely these objects are AM CVns than

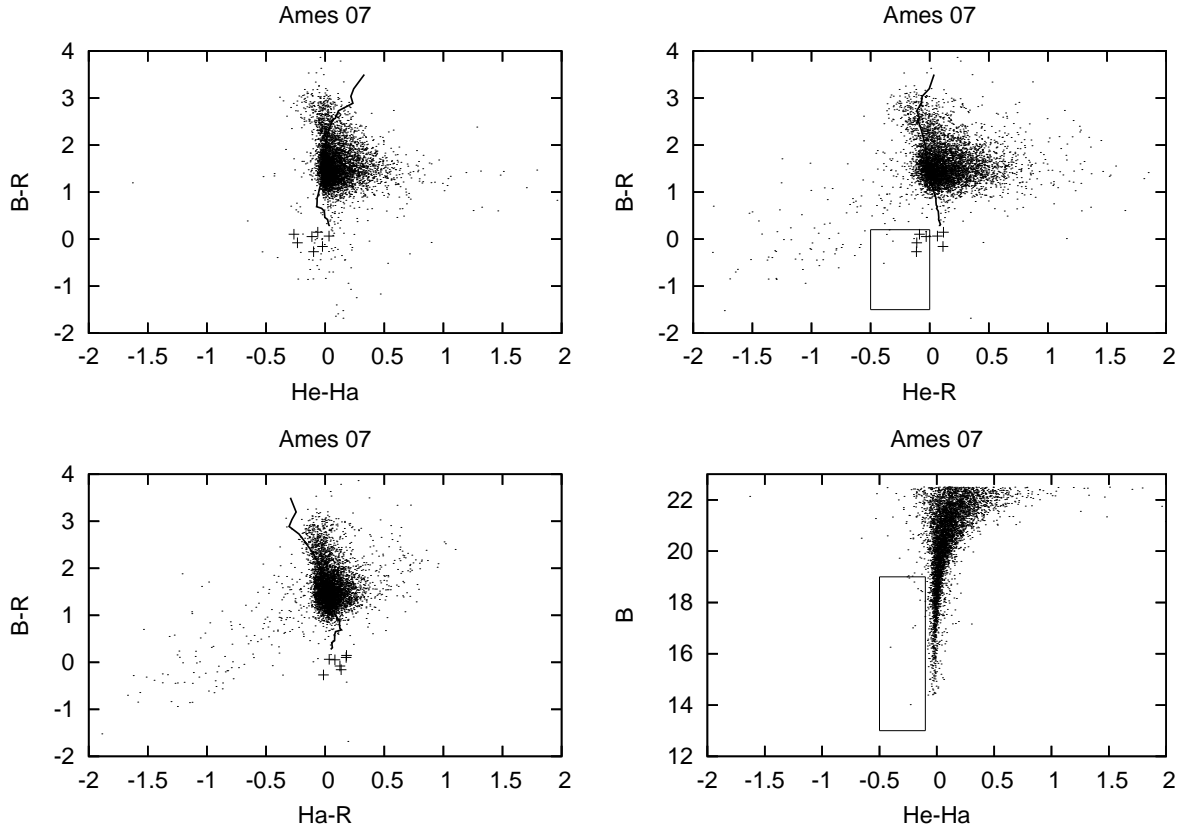


Figure 5.1. Colour-colour diagrams of field Ames 07. The selection boxes can be seen in the He-R versus B-R and He-Ha versus B diagrams.

those in category A, they are still interesting. In category C we have objects that are almost certainly not AM CVns, but can still be of interest. They are objects inside the box in the He-R versus B-R diagram that have He-Ha larger than zero, so H-alpha emission. The final category, category D, are objects with B-R smaller than zero, and either Ha-R or He-R different from zero (at least 0.1, at most 0.3). These are blue objects that have some feature in Helium or H-alpha. Basically these are a last grab to see if we can find anything interesting in this group, because any feature in Helium or H-alpha means the objects is not a main sequence star.

5.2 The selected objects

C++ programs were written to easily select the interesting objects and divide them into the above categories. For each field lists were made of the IDs of the objects in each category. These could then be combined into a master list, and the corresponding magnitudes and coordinates could be easily looked up. For the complete list, see the Appendix. Suffice to say we found 15 candidates in category A, 166 candidates in category B, 37 candidates in category C and 45 candidates in Category D. The 15 category A candidates are of course the most interesting, since these are the most likely candidates for AM CVns. Of these 15, 4 are also category D candidates, which makes them even more likely to be AM CVns.

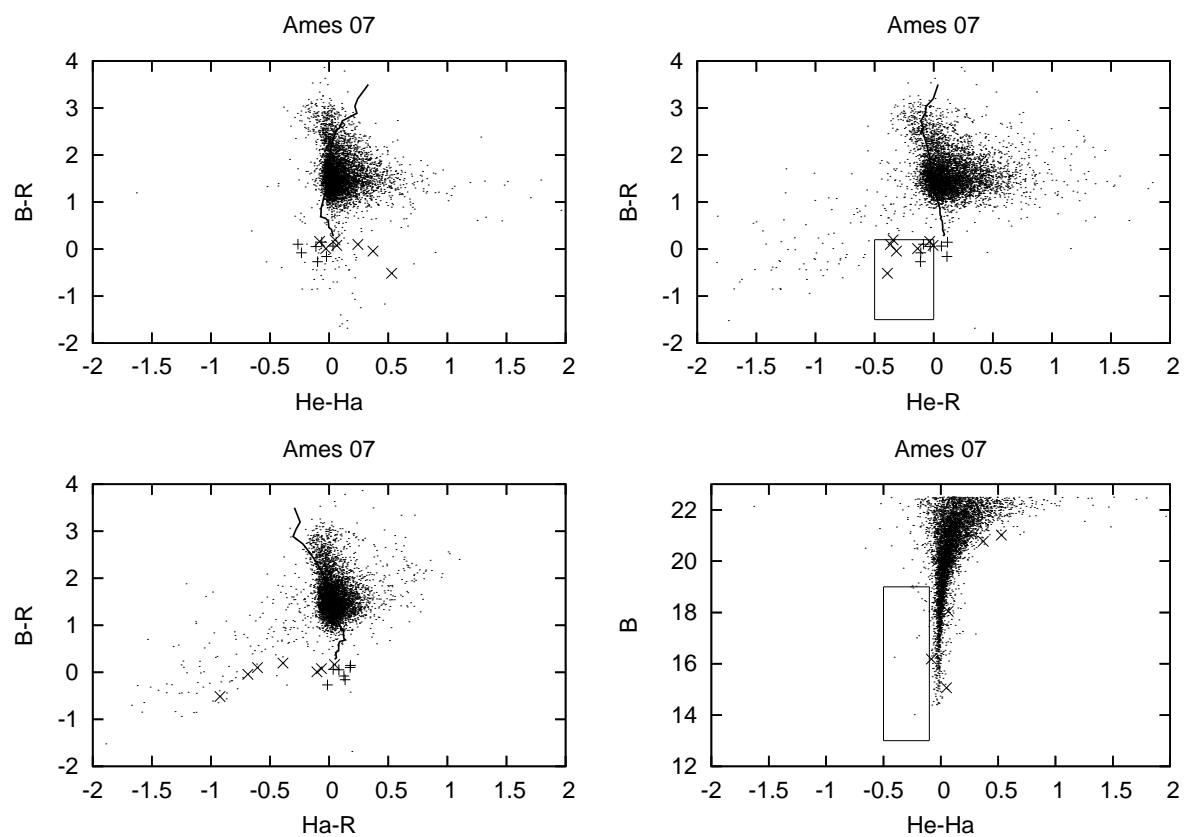


Figure 5.2. Colour-colour diagrams of field Ames 07. The plusses are the known AMCVn's, the crosses are the objects inside the box in the He-R versus B-R diagram.

Further conclusions about the likelihood of the candidates to be AM CVns cannot be drawn with the data we have at our disposal in this research. This would require followup spectroscopic observations of the candidates.

The 15 category A candidates can be seen in the colour-colour diagrams along with the known AM CVns in Figure 5.3. Their coordinates and the magnitudes (with errors) for each filter can be viewed in Table 5.1.

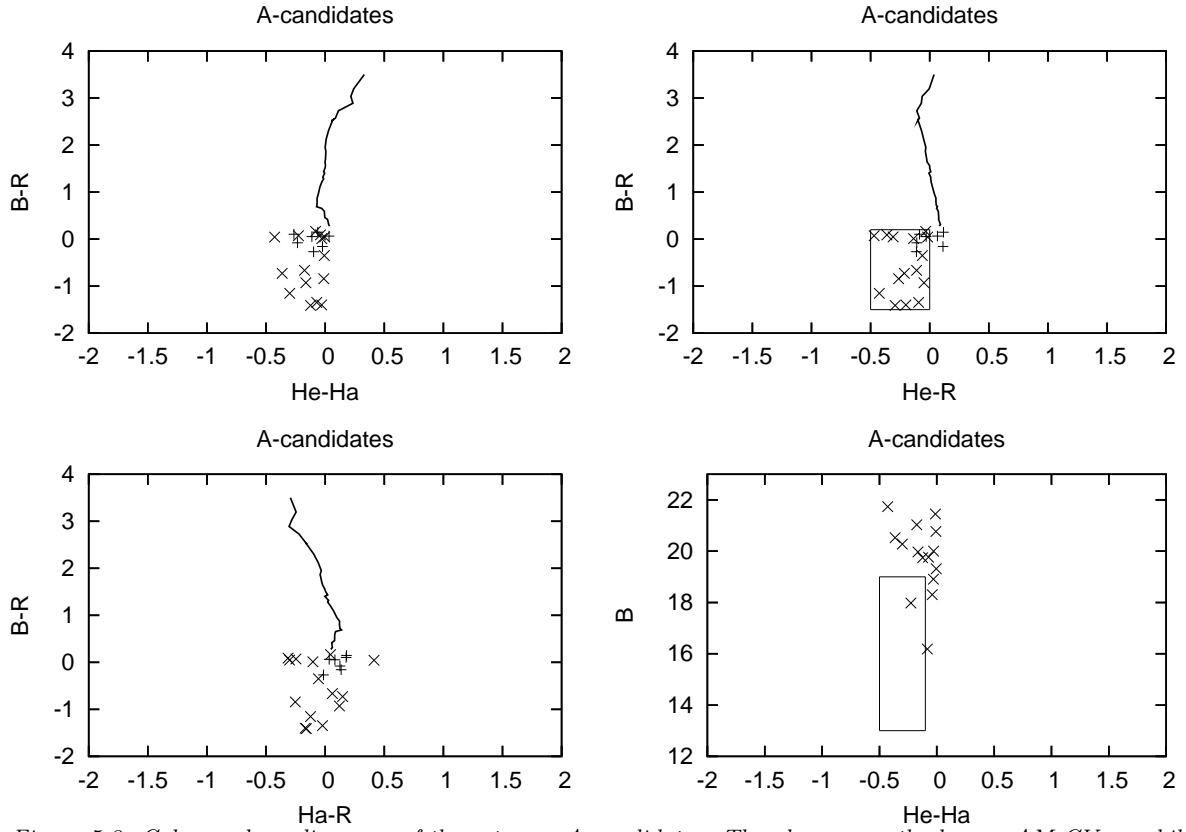


Figure 5.3. Colour-colour diagrams of the category A candidates. The plusses are the known AM CVns, while the diagonal crosses are the candidates of category A. The line is once again the theoretical main sequence.

Right Ascension	Declination	B	B-error	R	R-error	He	He-error	Ha	Ha-error
253.55	-8.83	20.00	0.01	19.98	0.02	-8.02	0.04	-8.56	0.03
253.06	-8.68	16.18	0.01	16.01	0.01	-11.91	0.01	-12.36	0.01
253.39	-6.49	20.52	0.01	21.25	0.04	-6.93	0.08	-7.12	0.08
253.14	-6.53	19.31	0.01	19.26	0.01	-8.96	0.02	-9.48	0.01
253.80	-9.07	18.90	0.01	20.31	0.02	-7.88	0.04	-8.44	0.03
253.86	-8.58	20.76	0.02	21.11	0.04	-6.90	0.08	-7.24	0.07
253.66	-7.28	19.76	0.01	21.10	0.04	-6.93	0.07	-7.32	0.06
254.01	-6.64	17.97	0.01	17.90	0.01	-10.41	0.01	-10.74	0.01
254.16	-6.31	19.96	0.01	20.89	0.04	-6.91	0.08	-7.27	0.07
254.55	-8.72	20.27	0.01	21.43	0.05	-7.08	0.07	-7.33	0.07
254.34	-9.03	21.03	0.02	21.69	0.06	-6.37	0.11	-6.73	0.09
254.62	-8.95	21.73	0.04	21.69	0.06	-6.10	0.12	-6.20	0.12
254.43	-6.86	19.74	0.01	21.15	0.05	-6.93	0.08	-7.35	0.07
255.01	-8.85	18.30	0.01	18.21	0.01	-10.20	0.01	-10.72	0.01
255.25	-5.81	21.44	0.03	22.28	0.09	-5.91	0.14	-6.46	0.12

Table 5.1. Coordinates and magnitudes (with errors) of all category A candidates. Numbers are rounded at two decimals.

Chapter 6

Conclusion

In this thesis we have used the Astro-WISE package to analyze a survey done to find AM CVn systems. The goal of this research was twofold. Firstly, it was meant to test the Astro-WISE system at the Radboud University in Nijmegen. Secondly, it was thought useful to check the data from the AM CVn survey again for AM CVn candidates. When testing the Astro-WISE system we focused on the speed, possibilities and user-friendliness of the system. Astro-WISE was able to perform most of the tasks quickly and efficiently. It also had most of the options we required and an interface that is relatively easy to use. There is a lot of room for improvement though. During the course of this research we encountered several bugs that slowed down the process, one of the most prominent ones being a database fault that can occur when handling large scripts. Also, exporting the data out of the Astro-WISE system proved not to be straightforward. We would have liked to see an easy-to-use webinterface to handle this sort of request, but the database viewer that is currently in use only allows for one object to be exported at the time, and is in general too complex. With a script of course the process becomes easily manageable. Apart from these types of setbacks however, the analysis process in Astro-WISE was fast and reliable. It takes some time to get familiar with the system, but no more than with any other software package. We conclude that the Astro-WISE system is ready to be used for other research, even though it is still in the development phase. More feedback from users should improve the system even further.

From the data in the AM CVn survey we gained a total of 15 promising AM CVn candidates. During the course of the analysis the only real problem we encountered was the occurrence of a strange 'tail' in some of the colour-colour diagrams created from the data. Fainter objects seem to be suffering from a shift in their magnitude in the redder filters. While we are unable to explain this phenomenon, we do not believe it makes the candidates we did find any less credible, since the bad fields have been left out of the analysis. To confirm whether the candidates we found are actually AM CVn stars, followup spectroscopy is needed.

Bibliography

An introduction to close binary stars, R.W. Hilditch, 2001

An introduction to the theory of stellar evolution, D. Prialnik, 2000

Separation of LISA Galactic and Extragalactic Signals, Hils D., Bender P.L., Stebbins R.T., 2000

Disk Instability Model for the AM Canum Venaticorum Stars, Tsugawa M., Osaki Y., 1997

Greenstein J.L., Matthews M.S., 1957, ApJ, 126, 14

Smak J., 1967, Acta Astron., 17, 255

Warner B., Robinson E.L., 1972, MNRAS, 159, 101

Nelemans G., Steeghs D., Groot P.J., 2001, MNRAS, 326, 621

AM CVn stars, Nelemans G., 2005

The chemical composition of donors in AM CVn stars and ultra-compact X-ray binaries: observational tests of their formation, Nelemans G., Yungelson L. R., van der Sluys M. V., Tout C. A., 2009

Appendix A

Astro-WISE scripts

In this appendix we will show four scripts for the Astro-WISE environment that were used during this research. Script A.1 can be used to create SourceLists from Regridded Frames, script A.2 to create SourceLists from Reduced Frames and script A.3 to create AssociateLists from SourceLists in four filters. Script A.4 was used to export AssociateLists from the Astro-WISE system.

```
for f in q:
    sl = SourceList()
    sl.frame = f
    sl.frame.retrieve()
    sl.frame.weight.retrieve()
    sl.make()
    sl.commit()
    os.system('rm *.fits')
    os.system('rm *.cat')
    os.system('rm tmp*')
```

Script A.1. An Astro-WISE script used to create SourceLists from Regridded Frames. Before using this script, one should have queried the desired Regridded Frames in a query called 'q'. Also note that this script removes all .fits, .cat and tmp files in the working dir of Astro-WISE, so make sure there are no important files of that type residing in the dir.

```
for f in q:
    astrom = (AstrometricParameters.reduced == f).max('creation_date')
    sl = SourceList()
    sl.frame = f
    sl.astrom_params = astrom
    sl.frame.retrieve()
    sl.frame.weight.retrieve()
    sl.make()
    sl.commit()
    os.system('rm *.fits')
    os.system('rm *.cat')
    os.system('rm tmp*')
```

Script A.2. An Astro-WISE script used to create SourceLists from Reduced Frames. Before using this script, one should have queried the desired Reduced Frames in a query called 'q'. Also note that this script removes all .fits, .cat and tmp files in the working dir of Astro-WISE, so make sure there are no important files of that type residing in the dir.

```

for sl in q:
    AL = AssociateList()
    s10 = sl
    s11 = ((SourceList.OBJECT==sl.OBJECT)&(SourceList.chip.name==sl.chip.name)&(SourceList.filter.name=='#844'))
    .max('creation_date')
    AL.input_lists.append(s10)
    AL.input_lists.append(s11)
    AL.set_search_distance(5.0)
    AL.make()
    AL.commit()
    ALs = (AssociateList.ALID==AL.ALID)[0]
    AL = AssociateList()
    SLs = ((SourceList.OBJECT==sl.OBJECT)&(SourceList.chip.name==sl.chip.name)&(SourceList.filter.name=='#865'))
    .max('creation_date')
    AL.input_lists.append(ALs)
    AL.input_lists.append(SLs)
    AL.make()
    AL.commit()
    ALs = (AssociateList.ALID==AL.ALID)[0]
    AL = AssociateList()
    SLs = ((SourceList.OBJECT==sl.OBJECT)&(SourceList.chip.name==sl.chip.name)&(SourceList.filter.name=='#858'))
    .max('creation_date')
    AL.input_lists.append(ALs)
    AL.input_lists.append(SLs)
    AL.make()
    AL.commit()

```

Script A.3. An Astro-WISE script used to create AssociateLists from SourceLists in four filters. Before using this script, one should have queried the desired SourceLists for one filter in a query called 'q'. The filter.name numbers in the script can be changed to the other three filters desired.

```

for al in q:
    attrlist = ['RA', 'DEC', 'MAG_ISO', 'MAGERR_ISO']
    r = al.associates.get_data(attrlist,mask=15,mode='ALL')
    f=file('AssociateList'+str(al.ALID), 'w')
    aids = [k for k in r.keys()]
    aids.sort()
    for aid in aids:
        for row in r[aid]:
            a=str(row)
            b=str(aid)
            c=str(al.ALID)
            f.write(a + c+'-'+b +'\n')
    f.close()

```

Script A.4. An Astro-WISE script used to export AssociateLists from the Astro-WISE system. It writes the Right Ascension, Declination, Magnitudes + errors and a source-specific ID to a file.

Appendix B

Candidate Lists

This appendix contains lists of all the Category A, B, C and D candidates, as outlined in chapter 5.

Right Ascension	Declination	B	B-error	R	R-error	He	He-error	Ha	Ha-error
253.55	-8.83	20.00	0.01	19.98	0.02	-8.02	0.04	-8.56	0.03
253.06	-8.68	16.18	0.01	16.01	0.01	-11.91	0.01	-12.36	0.01
253.39	-6.49	20.52	0.01	21.25	0.04	-6.93	0.08	-7.12	0.08
253.14	-6.53	19.31	0.01	19.26	0.01	-8.96	0.02	-9.48	0.01
253.80	-9.07	18.90	0.01	20.31	0.02	-7.88	0.04	-8.44	0.03
253.86	-8.58	20.76	0.02	21.11	0.04	-6.90	0.08	-7.24	0.07
253.66	-7.28	19.76	0.01	21.10	0.04	-6.93	0.07	-7.32	0.06
254.01	-6.64	17.97	0.01	17.90	0.01	-10.41	0.01	-10.74	0.01
254.16	-6.31	19.96	0.01	20.89	0.04	-6.91	0.08	-7.27	0.07
254.55	-8.72	20.27	0.01	21.43	0.05	-7.08	0.07	-7.33	0.07
254.34	-9.03	21.03	0.02	21.69	0.06	-6.37	0.11	-6.73	0.09
254.62	-8.95	21.73	0.04	21.69	0.06	-6.10	0.12	-6.20	0.12
254.43	-6.86	19.74	0.01	21.15	0.05	-6.93	0.08	-7.35	0.07
255.01	-8.85	18.30	0.01	18.21	0.01	-10.20	0.01	-10.72	0.01
255.25	-5.81	21.44	0.03	22.28	0.09	-5.91	0.14	-6.46	0.12

Table B.1. Coordinates and magnitudes (with errors) of all category A candidates. Numbers are rounded at two decimals.

Right Ascension	Declination	B	B-error	R	R-error	He	He-error	Ha	Ha-error
253.28	-8.60	18.02	0.01	17.74	0.01	-10.72	0.01	-11.00	0.01
253.18	-8.58	17.50	0.01	15.18	0.01	-13.14	0.01	-13.52	0.01
253.59	-8.47	18.60	0.01	18.17	0.01	-10.04	0.01	-10.38	0.01
253.49	-7.61	17.75	0.01	16.36	0.01	-11.71	0.01	-12.15	0.01
253.45	-7.78	18.08	0.01	17.28	0.01	-10.76	0.01	-11.17	0.01
253.52	-7.98	18.13	0.01	15.46	0.01	-12.56	0.01	-13.00	0.01
253.52	-7.96	18.69	0.01	21.28	0.01	-6.90	0.09	-7.21	0.07
253.55	-7.83	18.68	0.01	16.02	0.01	-11.84	0.01	-12.26	0.01
253.09	-7.10	18.47	0.01	15.95	0.01	-12.30	0.01	-12.64	0.01
253.24	-7.42	18.95	0.01	16.35	0.01	-11.99	0.01	-12.33	0.01
253.36	-6.47	18.88	0.01	16.22	0.01	-11.96	0.01	-12.37	0.01
253.31	-6.60	17.18	0.01	15.05	0.01	-12.99	0.01	-13.43	0.01
253.20	-6.50	17.48	0.01	15.35	0.01	-12.85	0.01	-13.20	0.01
253.37	-6.72	17.19	0.01	15.70	0.01	-12.36	0.01	-12.70	0.01
253.43	-6.67	17.59	0.01	16.57	0.01	-11.58	0.01	-11.89	0.01
253.48	-5.89	18.12	0.01	16.72	0.01	-11.36	0.01	-11.79	0.01
253.25	-5.99	16.80	0.01	14.85	0.01	-13.32	0.01	-13.65	0.01
253.07	-5.81	18.00	0.01	16.34	0.01	-11.71	0.01	-12.13	0.01
253.26	-6.24	16.46	0.01	13.83	0.01	-14.26	0.01	-14.65	0.01
253.44	-6.32	18.62	0.01	16.70	0.01	-11.53	0.01	-11.81	0.01
253.45	-6.23	18.48	0.01	17.57	0.01	-10.78	0.01	-11.13	0.01
253.44	-6.17	18.84	0.01	17.92	0.01	-10.24	0.01	-10.65	0.01
253.52	-6.21	18.67	0.01	16.98	0.01	-10.79	0.01	-11.09	0.01
253.51	-6.16	16.83	0.01	14.97	0.01	-12.97	0.01	-13.38	0.01
254.13	-8.73	18.47	0.01	16.68	0.01	-11.23	0.01	-11.37	0.01
253.75	-8.79	18.26	0.01	16.42	0.01	-11.49	0.01	-11.94	0.01
253.69	-8.72	17.97	0.01	17.08	0.01	-11.28	0.01	-11.69	0.01
253.70	-8.71	18.58	0.01	15.73	0.01	-12.21	0.01	-12.56	0.01
253.64	-8.64	18.66	0.01	16.62	0.01	-11.37	0.01	-11.84	0.01
253.70	-8.65	18.90	0.01	17.88	0.01	-10.31	0.01	-10.78	0.01
253.62	-9.07	18.54	0.01	16.10	0.01	-12.15	0.01	-12.55	0.01
253.63	-9.01	16.72	0.01	14.85	0.01	-13.12	0.01	-13.58	0.01
253.82	-8.93	18.35	0.01	17.30	0.01	-11.13	0.01	-11.44	0.01
253.83	-8.92	17.27	0.01	14.71	0.01	-13.28	0.01	-13.74	0.01
254.01	-9.06	18.64	0.01	16.03	0.01	-11.90	0.01	-12.20	0.01
254.04	-9.08	16.16	0.01	13.82	0.01	-14.13	0.01	-14.61	0.01
253.99	-8.30	18.97	0.01	17.13	0.01	-10.80	0.01	-11.04	0.01
253.75	-8.32	18.97	0.01	16.75	0.01	-11.22	0.01	-11.24	0.01
253.73	-8.33	18.72	0.01	16.21	0.01	-11.71	0.01	-11.70	0.01
253.67	-8.08	17.74	0.01	14.20	0.01	-13.96	0.01	-14.00	0.01
253.64	-8.40	18.59	0.01	17.26	0.01	-11.04	0.01	-11.24	0.01
253.87	-8.42	16.80	0.01	13.98	0.01	-14.08	0.01	-14.15	0.01
253.81	-8.39	17.82	0.01	15.31	0.01	-12.79	0.01	-12.92	0.01
254.01	-8.49	18.96	0.01	17.97	0.01	-10.32	0.01	-10.36	0.01
254.08	-7.65	16.85	0.01	13.59	0.01	-14.42	0.01	-14.94	0.01
253.80	-7.76	18.74	0.01	18.11	0.01	-9.90	0.01	-10.55	0.01
253.81	-7.61	16.64	0.01	13.98	0.01	-14.09	0.01	-14.69	0.01
253.86	-7.56	14.48	0.01	13.44	0.01	-14.52	0.01	-14.90	0.01
253.68	-7.72	18.94	0.01	17.89	0.01	-10.10	0.01	-10.63	0.01
253.68	-7.67	18.88	0.01	15.92	0.01	-12.29	0.01	-12.86	0.01
253.68	-7.66	18.93	0.01	16.09	0.01	-12.10	0.01	-12.73	0.01
253.65	-7.88	15.18	0.01	13.60	0.01	-14.44	0.01	-14.99	0.01
253.66	-7.80	15.64	0.01	13.57	0.01	-14.48	0.01	-14.95	0.01
254.17	-8.03	16.71	0.01	15.42	0.01	-12.48	0.01	-13.16	0.01
254.06	-7.92	18.09	0.01	15.52	0.01	-12.57	0.01	-13.15	0.01
254.17	-7.16	18.97	0.01	17.97	0.01	-10.38	0.01	-10.76	0.01
254.14	-7.10	17.54	0.01	15.30	0.01	-12.86	0.01	-13.15	0.01

Right Ascension	Declination	B	B-error	R	R-error	He	He-error	Ha	Ha-error
253.97	-7.04	18.90	0.01	17.36	0.01	-10.75	0.01	-11.10	0.01
253.94	-7.04	18.73	0.01	17.20	0.01	-10.88	0.01	-11.25	0.01
253.71	-7.01	18.16	0.01	20.48	0.03	-7.61	0.05	-7.89	0.05
254.16	-7.41	18.43	0.01	17.25	0.01	-10.49	0.01	-10.72	0.01
254.13	-6.54	18.72	0.01	17.94	0.01	-9.95	0.01	-10.11	0.01
254.02	-6.51	17.65	0.01	16.44	0.01	-11.66	0.01	-11.88	0.01
253.99	-6.43	17.14	0.01	14.82	0.01	-13.70	0.01	-13.90	0.01
253.77	-6.60	18.92	0.01	16.88	0.01	-11.38	0.01	-11.74	0.01
253.67	-6.49	16.93	0.01	15.14	0.01	-12.83	0.01	-13.23	0.01
253.70	-6.44	18.02	0.01	15.56	0.01	-12.72	0.01	-13.11	0.01
253.84	-6.85	17.73	0.01	15.48	0.01	-12.67	0.01	-13.10	0.01
253.81	-6.68	17.23	0.01	16.12	0.01	-12.04	0.01	-12.40	0.01
254.00	-6.78	18.49	0.01	16.64	0.01	-11.27	0.01	-11.48	0.01
254.00	-6.75	17.45	0.01	14.98	0.01	-12.91	0.01	-13.33	0.01
253.98	-6.66	18.98	0.01	17.78	0.01	-10.36	0.01	-10.82	0.01
254.01	-6.64	17.97	0.01	17.90	0.01	-10.41	0.01	-10.74	0.01
254.08	-6.87	17.91	0.01	15.56	0.01	-12.53	0.01	-12.95	0.01
254.04	-6.86	18.36	0.01	15.89	0.01	-12.13	0.01	-12.55	0.01
254.04	-6.79	18.83	0.01	16.30	0.01	-11.72	0.01	-12.09	0.01
254.15	-6.76	18.37	0.01	17.33	0.01	-10.74	0.01	-11.00	0.01
254.14	-5.91	18.83	0.01	16.38	0.01	-11.71	0.01	-12.05	0.01
254.04	-5.90	18.99	0.01	17.60	0.01	-10.37	0.01	-10.75	0.01
253.92	-6.04	18.59	0.01	16.14	0.01	-12.11	0.01	-12.48	0.01
253.90	-6.01	16.94	0.01	14.76	0.01	-13.50	0.01	-13.92	0.01
253.95	-5.89	18.86	0.01	16.49	0.01	-11.84	0.01	-12.23	0.01
253.95	-5.84	17.38	0.01	15.26	0.01	-13.14	0.01	-13.53	0.01
253.72	-6.20	18.42	0.01	15.57	0.01	-12.40	0.01	-12.58	0.01
253.63	-6.07	18.86	0.01	16.54	0.01	-11.70	0.01	-12.04	0.01
253.61	-6.11	18.05	0.01	16.79	0.01	-11.24	0.01	-11.59	0.01
253.77	-6.10	17.63	0.01	15.33	0.01	-12.86	0.01	-13.21	0.01
254.10	-6.32	15.38	0.01	14.11	0.01	-13.81	0.01	-14.22	0.01
254.51	-8.88	16.51	0.01	14.98	0.01	-13.52	0.01	-13.70	0.01
254.48	-8.80	17.94	0.01	15.60	0.01	-12.68	0.01	-13.06	0.01
254.42	-8.73	17.96	0.01	16.61	0.01	-11.65	0.01	-12.07	0.01
254.30	-8.86	16.95	0.01	14.66	0.01	-13.43	0.01	-13.79	0.01
254.32	-8.85	17.86	0.01	15.67	0.01	-12.30	0.01	-12.53	0.01
254.47	-9.02	18.64	0.01	17.09	0.01	-10.97	0.01	-11.17	0.01
254.34	-8.37	18.78	0.01	16.22	0.01	-11.87	0.01	-12.32	0.01
254.66	-8.48	18.58	0.01	16.07	0.01	-11.87	0.01	-12.29	0.01
254.58	-7.74	17.10	0.01	14.74	0.01	-13.30	0.01	-13.60	0.01
254.67	-6.93	18.92	0.01	16.33	0.01	-11.88	0.01	-12.30	0.01
254.24	-7.13	18.10	0.01	16.66	0.01	-11.79	0.01	-12.20	0.01
254.14	-7.10	17.61	0.01	15.24	0.01	-13.13	0.01	-13.35	0.01
254.38	-6.51	18.48	0.01	17.41	0.01	-10.52	0.01	-10.94	0.01
254.33	-6.43	18.49	0.01	16.14	0.01	-11.93	0.01	-12.35	0.01
254.32	-6.40	18.55	0.01	16.21	0.01	-11.99	0.01	-12.33	0.01
254.28	-6.71	17.12	0.01	14.79	0.01	-13.39	0.01	-13.74	0.01
254.54	-6.83	18.31	0.01	16.02	0.01	-12.07	0.01	-12.46	0.01
254.46	-6.64	18.99	0.01	16.51	0.01	-11.49	0.01	-11.82	0.01
254.62	-6.69	18.54	0.01	16.13	0.01	-11.86	0.01	-12.21	0.01
254.48	-5.93	17.92	0.01	15.39	0.01	-12.73	0.01	-13.18	0.01
254.39	-5.99	18.57	0.01	16.23	0.01	-11.90	0.01	-12.25	0.01
254.14	-5.91	18.90	0.01	16.48	0.01	-11.85	0.01	-12.14	0.01
254.16	-6.25	17.24	0.01	14.33	0.01	-13.80	0.01	-14.12	0.01
254.16	-6.15	18.97	0.01	16.40	0.01	-11.57	0.01	-11.99	0.01
254.35	-6.26	17.88	0.01	15.56	0.01	-12.78	0.01	-13.08	0.01
254.30	-6.17	17.78	0.01	16.34	0.01	-12.10	0.01	-12.48	0.01

Right Ascension	Declination	B	B-error	R	R-error	He	He-error	Ha	Ha-error
254.29	-6.14	18.65	0.01	17.58	0.01	-10.91	0.01	-11.33	0.01
254.33	-6.12	17.90	0.01	15.25	0.01	-12.77	0.01	-13.20	0.01
254.38	-6.12	17.14	0.01	14.61	0.01	-13.42	0.01	-13.79	0.01
254.53	-6.23	15.32	0.01	12.72	0.01	-15.44	0.01	-15.86	0.01
255.25	-8.78	18.88	0.01	16.20	0.01	-11.70	0.01	-12.15	0.01
255.04	-8.79	18.89	0.01	16.40	0.01	-11.81	0.01	-12.26	0.01
255.07	-8.74	16.28	0.01	14.11	0.01	-14.22	0.01	-14.53	0.01
255.11	-8.67	15.72	0.01	13.20	0.01	-15.06	0.01	-15.46	0.01
254.85	-8.82	17.03	0.01	15.40	0.01	-12.48	0.01	-12.90	0.01
254.98	-8.76	14.60	0.01	12.63	0.01	-15.26	0.01	-15.69	0.01
254.79	-8.88	18.78	0.01	16.83	0.01	-11.25	0.01	-11.46	0.01
254.79	-8.86	16.94	0.01	14.64	0.01	-13.73	0.01	-14.02	0.01
254.77	-8.83	17.43	0.01	15.98	0.01	-11.99	0.01	-12.37	0.01
254.76	-8.82	18.79	0.01	17.01	0.01	-11.12	0.01	-11.28	0.01
254.82	-8.82	18.35	0.01	17.21	0.01	-10.80	0.01	-11.20	0.01
254.81	-8.75	17.93	0.01	16.26	0.01	-11.71	0.01	-12.13	0.01
254.93	-9.15	18.76	0.01	16.94	0.01	-11.09	0.01	-11.53	0.01
254.86	-9.06	18.26	0.01	16.40	0.01	-11.58	0.01	-11.87	0.01
254.87	-9.01	17.01	0.01	16.27	0.01	-11.97	0.01	-12.41	0.01
254.98	-8.96	16.71	0.01	14.36	0.01	-13.84	0.01	-14.26	0.01
255.01	-8.97	18.60	0.01	16.00	0.01	-12.02	0.01	-12.38	0.01
255.05	-8.95	17.57	0.01	15.17	0.01	-12.81	0.01	-13.19	0.01
255.11	-8.94	16.69	0.01	15.92	0.01	-12.09	0.01	-12.50	0.01
255.25	-9.04	15.85	0.01	13.06	0.01	-14.70	0.01	-15.03	0.01
255.11	-8.23	16.23	0.01	13.06	0.01	-14.92	0.01	-15.62	0.01
255.08	-8.23	15.37	0.01	14.08	0.01	-14.22	0.01	-14.75	0.01
255.04	-8.14	18.81	0.01	16.70	0.01	-11.67	0.01	-12.18	0.01
254.91	-8.10	18.77	0.01	17.22	0.01	-10.91	0.01	-11.57	0.01
254.82	-8.31	18.99	0.01	17.61	0.01	-10.58	0.01	-11.24	0.01
254.79	-8.27	18.38	0.01	16.04	0.01	-12.12	0.01	-12.82	0.01
254.83	-8.11	18.97	0.01	15.26	0.01	-12.99	0.01	-13.43	0.01
254.79	-8.08	18.06	0.01	16.72	0.01	-11.43	0.01	-12.11	0.01
254.74	-8.56	13.83	0.01	12.29	0.01	-15.72	0.01	-16.17	0.01
254.76	-8.47	17.62	0.01	15.99	0.01	-12.31	0.01	-13.01	0.01
254.88	-8.50	17.34	0.01	15.25	0.01	-13.01	0.01	-13.71	0.01
254.91	-8.47	14.62	0.01	13.60	0.01	-14.77	0.01	-15.48	0.01
254.93	-8.44	14.86	0.01	14.05	0.01	-14.30	0.01	-14.98	0.01
255.11	-8.47	17.91	0.01	16.72	0.01	-11.44	0.01	-12.17	0.01
255.19	-8.42	15.62	0.01	14.16	0.01	-13.98	0.01	-14.66	0.01
255.26	-8.39	18.03	0.01	17.17	0.01	-10.71	0.01	-11.40	0.01
255.14	-7.55	15.85	0.01	14.19	0.01	-13.98	0.01	-14.78	0.01
254.82	-7.52	15.02	0.01	13.09	0.01	-15.23	0.01	-15.95	0.01
255.08	-8.00	16.91	0.01	14.00	0.01	-14.40	0.01	-15.12	0.01
254.83	-5.92	18.38	0.01	15.96	0.01	-12.18	0.01	-12.54	0.01
254.71	-6.25	16.76	0.01	14.33	0.01	-13.99	0.01	-14.33	0.01
254.79	-6.19	17.71	0.01	15.40	0.01	-12.84	0.01	-13.16	0.01
255.04	-6.29	18.23	0.01	15.74	0.01	-12.45	0.01	-12.88	0.01
255.12	-6.26	18.69	0.01	17.49	0.01	-10.92	0.01	-11.00	0.01
255.19	-6.21	17.99	0.01	15.57	0.01	-12.45	0.01	-12.85	0.01
255.69	-7.73	18.49	0.01	17.10	0.01	-11.31	0.01	-11.42	0.01
255.52	-7.54	18.20	0.01	15.85	0.01	-12.49	0.01	-12.56	0.01
255.39	-7.84	18.76	0.01	16.02	0.01	-12.13	0.01	-12.43	0.01

Table B.2. Coordinates and magnitudes (with errors) of all category B candidates. Numbers are rounded at two decimals.

Right Ascension	Declination	B	B-error	R	R-error	He	He-error	Ha	Ha-error
253.50	-8.77	18.04	0.01	17.96	0.01	-9.91	0.01	-10.55	0.01
253.07	-8.89	20.77	0.02	20.81	0.03	-7.39	0.06	-8.29	0.03
253.16	-9.02	15.06	0.01	14.86	0.01	-13.39	0.01	-13.99	0.01
253.28	-9.03	21.01	0.02	21.52	0.05	-6.84	0.08	-7.92	0.05
253.44	-9.16	21.06	0.03	20.96	0.03	-7.28	0.06	-8.09	0.04
253.39	-8.40	21.64	0.04	21.56	0.05	-6.80	0.08	-7.60	0.06
253.44	-7.24	20.26	0.01	20.16	0.02	-7.82	0.04	-8.60	0.03
253.44	-7.25	19.87	0.01	19.97	0.02	-8.40	0.03	-9.17	0.02
254.07	-8.74	15.50	0.01	15.48	0.01	-12.83	0.01	-13.92	0.03
254.10	-8.72	16.26	0.01	16.86	0.01	-11.51	0.01	-12.87	0.01
254.01	-8.95	18.40	0.01	18.28	0.01	-10.10	0.01	-11.27	0.01
254.16	-8.95	21.34	0.03	21.34	0.05	-6.84	0.08	-7.49	0.06
254.15	-6.47	18.63	0.01	18.96	0.01	-9.12	0.02	-9.84	0.01
254.01	-6.23	21.35	0.03	21.28	0.05	-6.88	0.08	-7.51	0.06
254.65	-8.89	17.83	0.01	18.11	0.01	-10.02	0.01	-11.27	0.01
254.28	-8.83	20.07	0.01	19.91	0.02	-8.16	0.03	-9.04	0.02
254.28	-8.81	19.60	0.01	19.55	0.01	-8.60	0.03	-9.64	0.01
254.24	-8.86	20.77	0.02	21.33	0.05	-6.67	0.09	-7.25	0.07
254.26	-9.13	17.63	0.01	18.13	0.01	-9.98	0.01	-11.45	0.01
254.65	-8.96	16.20	0.01	17.29	0.01	-10.73	0.01	-12.80	0.01
254.65	-8.33	20.81	0.02	20.91	0.04	-7.34	0.06	-7.96	0.04
254.63	-8.32	20.87	0.02	20.68	0.03	-7.15	0.07	-8.07	0.04
254.63	-8.26	20.92	0.02	21.68	0.06	-6.21	0.12	-7.54	0.05
254.33	-8.22	20.54	0.01	20.36	0.02	-7.48	0.05	-8.10	0.03
254.18	-8.34	16.55	0.01	16.48	0.01	-11.88	0.01	-12.48	0.01
254.55	-8.36	20.66	0.02	21.27	0.04	-6.90	0.08	-7.81	0.04
254.69	-8.41	18.86	0.01	19.00	0.01	-9.22	0.02	-9.83	0.01
254.53	-6.21	21.92	0.04	21.81	0.06	-6.28	0.11	-7.11	0.07
255.04	-8.96	20.53	0.02	20.47	0.03	-7.66	0.05	-8.32	0.03
254.85	-8.28	22.17	0.06	23.18	0.16	-5.00	0.20	-7.93	0.05
254.82	-8.30	20.17	0.02	20.76	0.04	-7.50	0.06	-8.49	0.03
254.72	-8.53	21.63	0.05	22.42	0.11	-5.78	0.18	-7.84	0.05
254.77	-8.52	21.83	0.05	21.82	0.08	-6.18	0.12	-8.09	0.04
255.19	-8.55	21.82	0.05	22.89	0.13	-5.14	0.20	-7.82	0.05
255.12	-7.79	20.24	0.02	20.06	0.02	-8.52	0.03	-9.64	0.01
255.79	-7.61	20.05	0.01	20.55	0.03	-7.40	0.06	-7.88	0.05
255.37	-7.99	20.33	0.02	21.77	0.06	-6.30	0.11	-6.76	0.09

Table B.3. Coordinates and magnitudes (with errors) of all category C candidates. Numbers are rounded at two decimals.

Right Ascension	Declination	B	B-error	R	R-error	He	He-error	Ha	Ha-error
253.52	-7.96	18.69	0.01	21.28	0.05	-6.90	0.09	-7.21	0.07
253.56	-6.57	20.73	0.02	20.93	0.04	-6.28	0.11	-7.37	0.06
253.53	-6.51	20.53	0.01	21.02	0.04	-6.77	0.09	-7.28	0.07
253.18	-6.39	21.15	0.02	21.93	0.06	-5.87	0.14	-6.61	0.09
253.18	-6.05	17.83	0.01	18.21	0.01	-9.59	0.01	-10.25	0.01
253.73	-8.80	19.24	0.01	21.97	0.07	-5.54	0.16	-6.22	0.11
253.85	-8.73	20.25	0.01	21.18	0.03	-6.55	0.09	-7.25	0.06
253.87	-8.68	22.09	0.05	22.23	0.07	-5.55	0.14	-5.82	0.13
253.66	-8.85	20.33	0.01	21.87	0.06	-6.16	0.12	-6.19	0.11
254.10	-7.66	21.28	0.03	21.52	0.05	-6.40	0.11	-7.52	0.06
254.15	-7.89	20.66	0.02	22.75	0.11	-9.84	0.01	-5.70	0.15
253.76	-7.91	19.28	0.01	21.59	0.05	-6.31	0.11	-7.35	0.06
253.80	-7.35	19.79	0.01	22.57	0.09	-5.94	0.14	-6.15	0.12
253.71	-7.01	18.16	0.01	20.48	0.03	-7.61	0.05	-7.89	0.05
253.68	-6.61	21.54	0.03	22.34	0.12	-4.50	0.29	-6.06	0.12
254.15	-6.47	18.63	0.01	18.96	0.01	-9.12	0.02	-9.84	0.01
253.86	-6.79	17.68	0.01	22.18	0.10	-5.90	0.15	-6.79	0.09
253.96	-6.83	19.97	0.01	21.98	0.09	-5.62	0.16	-6.43	0.11
254.00	-6.72	20.94	0.02	21.58	0.08	-5.97	0.14	-6.41	0.10
253.98	-5.96	19.13	0.01	19.16	0.01	-8.58	0.03	-9.20	0.02
253.63	-6.14	20.53	0.02	23.74	0.15	-5.97	0.13	-4.97	0.21
254.16	-6.31	19.96	0.01	20.89	0.04	-6.91	0.08	-7.27	0.07
253.77	-5.96	19.24	0.01	21.70	0.06	-6.03	0.12	-6.05	0.12
254.55	-8.72	20.27	0.01	21.43	0.05	-7.08	0.07	-7.33	0.07
254.29	-9.12	19.15	0.01	22.26	0.09	-5.13	0.20	-6.36	0.12
254.63	-8.85	21.17	0.03	21.83	0.07	-5.74	0.15	-8.06	0.04
254.29	-8.79	20.84	0.02	22.58	0.10	-5.15	0.18	-5.01	0.21
254.26	-9.13	17.63	0.01	18.13	0.01	-9.98	0.01	-11.45	0.01
254.16	-9.12	19.20	0.01	21.81	0.07	-6.02	0.13	-6.28	0.12
254.34	-9.03	21.03	0.02	21.69	0.06	-6.37	0.11	-6.73	0.09
254.65	-8.96	16.20	0.01	17.29	0.01	-10.73	0.01	-12.80	0.01
254.14	-7.45	19.31	0.01	21.39	0.05	-5.86	0.15	-6.81	0.10
254.44	-7.25	19.48	0.01	21.04	0.04	-6.42	0.10	-7.10	0.07
254.64	-7.27	20.72	0.02	21.53	0.05	-5.23	0.19	-6.55	0.10
254.14	-6.60	21.04	0.03	21.09	0.04	-6.06	0.13	-7.20	0.08
254.85	-8.86	20.38	0.02	21.55	0.05	-5.80	0.14	-6.71	0.09
254.85	-8.28	22.17	0.06	23.18	0.16	-5.00	0.20	-7.93	0.05
254.82	-8.30	20.17	0.02	20.76	0.04	-7.50	0.06	-8.49	0.03
254.73	-8.56	22.04	0.06	22.37	0.11	-5.31	0.20	-7.75	0.06
254.72	-8.53	21.63	0.05	22.42	0.11	-5.78	0.18	-7.84	0.05
254.77	-8.47	22.44	0.07	22.76	0.12	-5.09	0.20	-7.74	0.05
255.48	-7.54	20.24	0.02	22.17	0.08	-5.63	0.15	-5.92	0.14
255.37	-7.99	20.33	0.02	21.77	0.06	-6.30	0.11	-6.76	0.09

Table B.4. Coordinates and magnitudes (with errors) of all category D candidates. Numbers are rounded at two decimals.